NRL Report 6798

Image Enhancement with Prolate Spheroidal Wave Functions

HENRY A. BROWN

Tracking Branch
Radar Division

November 29, 1968

NAVAL RESEARCH LABORATORY
Washington, D.C.

This document has been approved for public release and sale; its distribution is unlimited.

CONTENTS

Abstract	ii
Problem Status	ii
Authorization	ii
INTRODUCTION	1
AN OBJECT AND FAR FIELD RELATIONSHIP	1
DIFFRACTION-LIMITED IMAGING	3
EXACT IMAGE RECONSTRUCTION	5
The Prolate Spheroidal Wave Functions	5
Reconstruction Using the Far Field	6
Reconstruction Using the Diffraction Image	7
IMAGE ENHANCEMENT OF TWO POINT SOURCES	9
THE POINT SPREAD FUNCTION	11
GENERATION OF THE WAVE FUNCTIONS	13
Legendre Polynomial Expansion	14
Power Series Expansion	18
Verification of Results	21
SUMMARY	22
ACKNOWLEDGMENTS	22
REFERENCES	23
APPENDIX A - The Coefficients of the Prolate Spheroidal Angle Function Legendre Polynomial Expansion	25
APPENDIX B - The Prolate Spheroidal Eigenvalues and Normalization Constants	37
APPENDIX C - The Coefficients of the Prolate Spheroidal Angle Function Power Series Expansion	41

ABSTRACT

If the electric field intensity in the Fraunhofer region of a one-dimensional radiating source can be represented as a finite Fourier transform of the source current, then the source current can be reconstructed exactly by using prolate spheroidal wave functions and a segment of either the far field or the diffraction-limited image for the noise-free case. An example of the image enhancement of this process is given for the case of two equal point sources, which are unresolved in the Rayleigh sense. The point response function of this process shows that the resolution cell extent can be readily reduced to less than 10% of the Rayleigh cell with only 20 degrees of enhancement processing. A method of generating the Legendre polynomial and power series expansions of the prolate spheroidal angle functions of the first kind and order zero, $S_{0n}(c, x)$, has been worked out in detail. The Legendre polynomial expansion coefficients for degrees $n = 0(1)40$ and the power series expansion coefficients for degrees $n = 0(1)36$ are tabulated for $c = 2$.

PROBLEM STATUS

This is an interim report; work on the problem is continuing.

AUTHORIZATION

NRL Problem R02-14
Project RF-001-02-41-4005

Manuscript submitted August 23, 1968.

IMAGE ENHANCEMENT WITH PROLATE SPHEROIDAL WAVE FUNCTIONS

INTRODUCTION

The problem of producing an image of a reflecting target or a radiating source of electromagnetic energy in a noise-free case can be mathematically formulated in either of two equivalent ways — by two consecutive Fourier integrals or by one convolution integral. In the first approach a Fourier transform of the target or source current yields the radiated far field, so that the inverse Fourier transform of the entire far field will yield the current distribution producing the field. However, in any real situation, only a segment of the far field is known, so that when the transform of this segment is taken, an imperfect replica of the object is formed. This replica, due to the finite extent of the imaging aperture, is called the diffraction-limited image of the object.

In the second formulation, the diffraction-limited image is given by the convolution of the object function (target or source current) with the point spread function of the imaging system. An analogous situation exists in signal theory, where the output of a low-pass network is the convolution of the impulse response function of the network with the time signal.

In each of these two formulations the far field or diffraction-limited image, which in the context of the problem under consideration may be detected by a sensor remote from the object, is known as a function of the desired quantity — the object function. In other words the mathematical problem is to determine the target current as an explicit function of the available information, i.e., a known segment of the far field or the diffraction-limited image, given the implicit relationship.

A special set of mathematical functions called prolate spheroidal wave functions have the useful properties of being the eigenvalues of the Fourier transform kernel and of being orthogonal and complete over a given finite interval as well as over the entire real line. Application of these properties to the imaging problem formulations mentioned above allows the object function to be written as an explicit function of either the far field or the diffraction-limited image, which are the presumed knowns.

In this report these two formulations of the imaging problem will be inverted by using the prolate spheroidal wave functions, and the special case of image reconstruction of two point sources which are unresolvable in the classical Rayleigh sense will be examined. Since there is a significant lack of these functions or their expansion coefficients in the literature, the procedure for generating the coefficients for two different expansions will be discussed in detail. Tabulations of these coefficients are given in the appendixes.

AN OBJECT AND FAR FIELD RELATIONSHIP

The current $I(z)$ in a linear element may be related to the electric field intensity $E(\phi)$ in the Fraunhofer or far field region (1) by

$$E(\phi) = \int_{-a/2}^{a/2} I(z)\, e^{j2\pi \frac{z}{\lambda} \sin \phi}\, dz . \tag{1}$$

The geometry of this relationship is shown in Fig. 1. There are several assumptions (2) which are implied in the simple relationship of Eq. (1): scalar field theory is assumed to apply, the medium between the source point z and the field point y is homogeneous, the current in the radiator is linearly polarized, the object dimension is large compared with a wavelength, and the range R from the radiator is large so that the field point is in the Fraunhofer region. Another condition which is often overlooked is that for Eq. (1) to apply rigorously, the phase variation across the linear element must be zero. This condition is so restrictive when application is made to practical problems that often it is ignored as an expediency to the analysis. Of course the specific application must be considered before the validity of any of the above assumptions can be supported, and the justification for ignoring the constant phase restriction must be made. Also the specific application determines the actual physical assignment of the variables in Eq. (1).

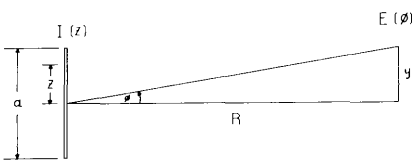

Fig. 1 - The geometrical relationship between the far field $E(\phi)$ and the current $I(z)$ in a linear element

Since the purpose of this study is to determine an explicit relationship for the object current rather than to delve into the applicability of Eq. (1) to all physical situations, statements of the above assumptions will suffice here as due caution against indiscriminantly using the far field and current relationship of Eq. (1).

To concentrate on the central problem of solving Eq. (1) for the current, the notation can be simplified by making the following substitutions. Let

$$\omega = \frac{2\pi}{\lambda} \sin \phi, \tag{2}$$

which is sometimes termed the spatial frequency, because its dimensions are radians per unit wavelength. If only small angles of ϕ are of interest, $\sin \phi$ can be approximated by y/R so that ω becomes $2\pi y/\lambda R$. Considering wavelength and range as constant parameters, ω can also be viewed as the distance variable in the far field just as z is the distance variable in the target. Restriction to small angles of ϕ, however, is not essential to the following formulations of the imaging problem, and the large-angle implications are discussed in another report (3). Also let $t = z$, so that at the endpoints of the linear element, $z = \pm a/2$, $t = \pm T/2$. Then the integral of Eq. (1) becomes

$$E(\omega) = \int_{-T/2}^{T/2} I(t)\, e^{j\omega t}\, dt\,. \tag{3}$$

In the parlance of signal theory the above integral expresses the frequency distribution of a time-limited signal $I(t)$. This integral has an inverse which is the Fourier transform

$$I(t) = \frac{1}{2\pi} \int_{-\infty}^{\infty} E(\omega)\, e^{-j\omega t}\, d\omega\,. \tag{4}$$

Physically, this means that the time-limited signal $I(t)$ may be reproduced exactly, if its entire frequency spectrum is known.

In terms of antenna theory the integral in Eq. (4) states that the current $I(t)$ may be determined exactly if the entire far field or radiation pattern of the antenna is known. In real situations, however, only a finite segment of the far field can be experimentally determined. This segment is often the extent that is contained within a finite receiving aperture. Herein, the problem lies. The target or antenna current must be reconstructed with a knowledge of the far field, only over a limited extent in space.

DIFFRACTION-LIMITED IMAGING

The integral relation in Eq. (4) will be termed the Fourier imaging integral, since it expresses the antenna current or object function $I(t)$ as the Fourier transform of the electric field intensity $E(\omega)$ in the Fraunhofer region. In all practical situations the far field is known only over a finite extent in space so that the reconstruction of the object function is necessarily imperfect. The reconstructed object function in this case is termed the diffraction-limited image, and the nature of this phenomenon as related to resolution can be easily demonstrated by a simple example.

Consider two in-phase, equal-amplitude isotropic point sources separated by a distance T. The far field radiated by these sources is simply

$$E(\omega) = \int_{-T/2}^{T/2} \left[\delta\left(t + \frac{T}{2}\right) + \delta\left(t - \frac{T}{2}\right)\right] e^{j\omega t}\, dt$$

$$= 2 \cos \frac{T}{2}\omega . \tag{5}$$

Suppose now that an aperture of total extent $2\omega_0$ contains the only knowledge of the far field. Then by the Fourier imaging integral in Eq. (4), the diffraction-limited image of these two point sources is

$$I'(t) = \frac{1}{2\pi} \int_{-\omega_0}^{\omega_0} 2 \cos \frac{T}{2}\omega\, e^{-j\omega t}\, d\omega$$

$$= \frac{\omega_0}{\pi} \frac{\sin \omega_0 T\left(\frac{t}{T} + \frac{1}{2}\right)}{\omega_0 T\left(\frac{t}{T} + \frac{1}{2}\right)} + \frac{\omega_0}{\pi} \frac{\sin \omega_0 T\left(\frac{t}{T} - \frac{1}{2}\right)}{\omega_0 T\left(\frac{t}{T} - \frac{1}{2}\right)} . \tag{6}$$

Hence, the image of two points is simply the sum of two $\sin x/x$ functions, as shown in Fig. 2, their peaks separated by T and each having a lobe width of $2\pi/\omega_0$. If the first null of one $\sin x/x$ function corresponds to the peak position of the other $\sin x/x$ function, the two points are said to be resolved in the Rayleigh sense. This condition of Rayleigh resolution occurs for $\omega_0 T = \pi$ and represents, in a practical sense, the smallest aperture $2\omega_0$ which can resolve two points separated by T for the case of Fourier imaging.

In the above discussion two steps were involved to produce the diffraction-limited image of the object function — an inverse Fourier transform to obtain the far field and a Fourier transform of a segment of this far field to obtain the image. Often, especially in the fields of optics and radio astronomy, the imaging process is represented by a single step involving convolution. Identical results to those shown above are, of course, obtained when the convolution representation is used.

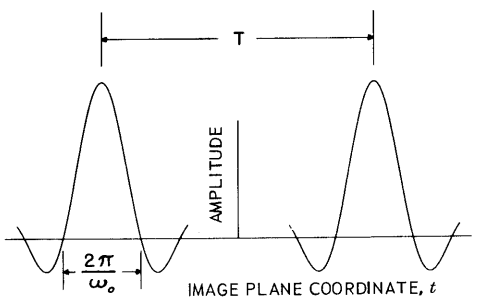

Fig. 2 - The diffraction-limited (Fourier) image of two equal phase and amplitude isotropic point sources (see Eq. (6))

Since the far field is known only over a segment of space $2\omega_0$, let $\Pi(\omega/\omega_0)$ be an aperture weighting function which is zero for $|\omega| > \omega_0$, which is unity for $|\omega| < \omega_0$. This function denotes no relative amplitude or phase weighting across the aperture. Now the imaging integral in Eq. (4) can be written with infinite limits, since the integrand is zero for $|\omega| > \omega_0$ as

$$I'(t) = \frac{1}{2\pi} \int_{-\infty}^{\infty} \Pi\left(\frac{\omega}{\omega_0}\right) E(\omega)\, e^{-j\omega t}\, d\omega\,, \tag{7}$$

which is the Fourier transform of the product of two functions. By the convolution theorem (4) the above integral is equal to the convolution of the Fourier transforms of each of the two factors Π and E. The transform of the aperture function Π is

$$\pi(t) = \frac{1}{2\pi} \int_{-\infty}^{\infty} \Pi\left(\frac{\omega}{\omega_0}\right) e^{-j\omega t}\, d\omega$$

$$= \frac{\omega_0}{\pi} \frac{\sin \omega_0 t}{\omega_0 t} \tag{8}$$

and the transform of E by Eq. (4) is the object function $I(t)$. Hence, the diffraction-limited image of $I(t)$ is

$$I'(t) = \frac{\omega_0}{\pi} \int_{-T/2}^{T/2} \frac{\sin \omega_0(t - t')}{\omega_0(t - t')}\, I(t')\, dt'\,. \tag{9}$$

The limits are finite because the object function is known to be zero outside the interval $|t'| < T/2$. The above integral states that the diffraction-limited image $I'(t)$ of an object function $I(t)$ is the convolution of the object function with a $\sin x/x$ function, which is the point spread function of a uniform aperture. For the case of the two equal point sources considered previously, substitution of the object function $I(t) = \delta(t \pm T/2)$ into the convolution integral in Eq. (9) leads to the identical results of Eq. (6) for the image produced by the two-step process of finding the far field and then taking a transform.

The convolution integral above gives the image $I'(t)$ as a function of the object $I(t)$ and the $\sin x/x$ point spread function. The central problem considered in this investigation is how to determine the object function given information measurable by a remote sensor. Hence, it is required that the above integral be solved explicitly for the object function $I(t)$ in terms of the remotely sensed image function $I'(t)$.

To solve Eq. (9) explicitly for the object function $I(t)$, the convolution theorem previously stated is applied with the results of Eq. (7). Taking the inverse of both sides of Eq. (7) yields

$$\int_{-\infty}^{\infty} I'(t)\, e^{j\omega t}\, dt = \Pi\left(\frac{\omega}{\omega_0}\right) \int_{-T/2}^{T/2} I(t)\, e^{j\omega t}\, dt\,. \tag{10}$$

If both sides of Eq. (10) could be divided by $\Pi(\omega/\omega_0)$ and the Fourier transform over $|\omega| < \infty$ taken again of both sides, the object function $I(t)$ would indeed be given explicitly as a function of the image $I'(t)$. However, this division is invalid since $\Pi(\omega/\omega_0)$ is zero outside the interval $|\omega| < \omega_0$. Taking finite limits for the transformation on both sides results in the identity of the diffraction-limited images $I'(t)$. However, it will be shown in the next section that both Eq. (3) for the far field and Eq. (9) for the image, each of which involve the object function implicitly, can be solved for the object function explicitly by the use of prolate spheroidal wave functions.

EXACT IMAGE RECONSTRUCTION

The Prolate Spheroidal Wave Functions

One of the eleven coordinate systems in which the scalar wave equation

$$(\nabla^2 + k^2)\,\psi = 0 \tag{11}$$

is separable is the prolate spheroidal system. This system can be formed by rotating the two-dimensional elliptic coordinate system consisting of confocal ellipses and hyperbolas about the major axis of the ellipses. By separation of variables the solution of Eq. (11) in this system is

$$\psi_{mn} = S_{mn}(c,\eta)\, R_{mn}(c,\xi) \begin{matrix}\cos\\ \sin\end{matrix}\, m\phi\,, \tag{12}$$

where S_{mn} and R_{mn} are the prolate angular and radial wave functions, respectively, of the first kind, order m, and degree n (5). The coordinates are (η, ξ, ϕ) and $c = kd/2$, where k is the constant in the wave equation and d is the interfocal distance. Although the geometry of the prolate spheroidal coordinate system is not of particular interest here, the above discussion explains the nomenclature for these functions.

The properties of these prolate spheroidal wave functions are discussed in detail by Slepian and Pollak (6), and those properties which are of particular application here are summarized in the equations below. Note that only order zero ($m = 0$) wave functions are used, the angle function contains the independent variable, and the radial function is evaluated at unity:

$$\int_{-\omega_0}^{\omega_0} S_{0n}\left(c, \frac{\omega}{\omega_0}\right)^{j\omega t} d\omega = 2 j^n \omega_0 R_{0n}(c,1)\; S_{0n}\left(c, \frac{2t}{T}\right), \tag{13}$$

$$\int_{-T/2}^{T/2} \frac{\sin \omega_0(t'-t)}{\omega_0(t'-t)}\, S_{0n}\left(c, \frac{2t}{T}\right) dt = T R_{0n}^2(c,1)\; S_{0n}\left(c, \frac{2t'}{T}\right), \tag{14}$$

$$\sum_{n=0}^{\infty} \frac{S_{0n}(c,x)\; S_{0n}\left(c, \frac{2t}{T}\right)}{N_n} = \delta\left(x - \frac{2t}{T}\right). \tag{15}$$

In the completeness relation in Eq. (15) the normalization factor is

$$N_n = \int_{-1}^{1} \left[S_{0n}(c, x) \right]^2 dx \tag{16}$$

and δ is the Dirac delta function. Two other properties of the angle functions $S_{0n}(c, x)$ which are of interest here are that S_{0n} is an even or odd function of x as the degree n is even or odd and that S_{0n} has exactly n zeroes in the interval $|x| \leq 1$. Most importantly, these functions are orthogonal and complete over both $|x| \leq 1$ and $|x| < \infty$. These properties will now be used to solve for the object $I(t)$ as an explicit function of either the far field $E(\omega)$ or the diffraction-limited image $I'(t)$.

Reconstruction Using the Far Field

The relationship between the far field and object function is

$$E(\omega) = \int_{-T/2}^{T/2} I(t) \; e^{j\omega t} \; dt , \tag{3}$$

where the object function is known to be zero outside $|t| = T/2$. This is to say that the object is known to be entirely included within the $|t| \leq T/2$ extent.

Multiplying by $S_{0n}(c, \omega/\omega_0)$ and integrating over the finite range $|\omega| < \omega_0$, in which the far field is known, gives

$$\int_{-\omega_0}^{\omega_0} E(\omega) \; S_{0n}\left(c, \frac{\omega}{\omega_0}\right) d\omega = \int_{-\omega_0}^{\omega_0} S_{0n}\left(c, \frac{\omega}{\omega_0}\right) \left[\int_{-T/2}^{T/2} I(t) \; e^{j\omega t} \; dt \right] d\omega . \tag{17}$$

Consider now only the right-hand side of the above equation. Since the integrands are analytic, the orders of integration may be interchanged to give

$$\int_{-T/2}^{T/2} I(t) \left[\int_{-\omega_0}^{\omega_0} S_{0n}\left(c, \frac{\omega}{\omega_0}\right) e^{j\omega t} \; d\omega \right] dt . \tag{18}$$

From the property of the angle functions as expressed by Eq. (13), the inner integral reduces the above to

$$2j^n \omega_0 R_{0n}(c, 1) \int_{-T/2}^{T/2} I(t) \; S_{0n}\left(c, \frac{2t}{T}\right) dt . \tag{19}$$

Dividing both sides of Eq. (17) by $2j^n \omega_0 R_{0n}$ yields

$$\int_{-\omega_0}^{\omega_0} \frac{E(\omega) \; S_{0n}\left(c, \frac{\omega}{\omega_0}\right)}{2j^n \omega_0 R_{0n}(c, 1)} \; d\omega = \int_{-T/2}^{T/2} I(t) \; S_{0n}\left(c, \frac{2t}{T}\right) dt . \tag{20}$$

Multiplying the above equation by $S_{0n}(c, x)/N_n$ and summing over all n gives

$$\sum_{n=0}^{\infty} \frac{S_{0n}(c,x)}{N_n} \int_{-\omega_0}^{\omega_0} \frac{E(\omega)\ S_{0n}\left(c, \frac{\omega}{\omega_0}\right)}{2j^n \omega_0 R_{0n}(c,1)}\, d\omega = \sum_{n=0}^{\infty} \frac{S_{0n}(c,x)}{N_n} \int_{-T/2}^{T/2} I(t)\ S_{0n}\left(c, \frac{2t}{T}\right) dt\ . \tag{21}$$

Interchanging the orders of integration and summation on the right yields

$$\int_{-T/2}^{T/2} I(t) \sum_{n=0}^{\infty} \frac{S_{0n}(c,x)\ S_{0n}\left(c, \frac{2t}{T}\right)}{N_n}\, dt, \tag{22}$$

which by the completeness property in Eq. (15) reduces the above to

$$\int_{-T/2}^{T/2} I(t)\ \delta\left(x - \frac{2t}{T}\right) dt = I\left(\frac{T}{2}x\right). \tag{23}$$

Returning to the left-hand side of Eq. (21) and defining

$$E_n = \int_{-\omega_0}^{\omega_0} \frac{E(\omega)\ S_{0n}\left(c, \frac{\omega}{\omega_0}\right)}{2j^n \omega_0 N_n R_{0n}(c,1)}\, d\omega, \tag{24}$$

we have the desired relationship for the object function as

$$\sum_{n=0}^{\infty} S_{0n}(c,x)\ E_n = I\left(\frac{T}{2}x\right). \tag{25}$$

This relationship states that given only a segment, $|\omega| < \omega_0$ and ω_0 arbitrary, of the far field $E(\omega)$ from an object existing within some extent T in space, that object $I(t)$ may be reconstructed exactly. It should be remembered that the Fourier imaging integral in Eq. (4) gives the diffraction-limited image, which is only an approximation to the object function when only a segment of the far field is known. Of course, for exact reconstruction the far field must be known exactly (no noise) over some $|\omega| < \omega_0$, and an infinite number of wave functions must be employed. Compromising either of these requirements will again lead to an approximation of the object function. The theoretical predictions of the degradations of noise on this reconstruction scheme are somewhat pessimistic (7,8) and will not be examined here. The effect of truncating this scheme to a finite number of degrees will be illustrated by example in the following section.

Reconstruction Using the Diffraction Image

The relationship in Eq. (9) between the diffraction-limited image $I'(t)$ and the object function $I(t')$

$$I'(t) = \frac{\omega_0}{\pi} \int_{-T/2}^{T/2} \frac{\sin\ \omega_0(t-t')}{\omega_0(t-t')}\ I(t')\, dt' \tag{9}$$

can be solved in an analogous manner explicitly for the object function. Multiplying by $S_{0n}(c, 2t/T)$ and integrating over the finite extent $|t| < T/2$ in which the target is known to exist gives

$$\int_{-T/2}^{T/2} I'(t)\ S_{0n}\left(c, \frac{2t}{T}\right) dt = \frac{\omega_0}{\pi} \int_{-T/2}^{T/2} S_{0n}\left(c, \frac{2t}{T}\right) \left[\int_{-T/2}^{T/2} \frac{\sin\ \omega_0(t-t')}{\omega_0(t-t')}\ I(t')\, dt'\right] dt\ . \tag{26}$$

Consider now only the right-hand side of the above equation. Since the integrands are continuous, the orders of integration may be interchanged to give

$$\frac{\omega_0}{\pi} \int_{-T/2}^{T/2} I(t') \left[\int_{-T/2}^{T/2} \frac{\sin\ \omega_0(t-t')}{\omega_0(t-t')}\ S_{0n}\left(c, \frac{2t}{T}\right) dt\right] dt'\ . \tag{27}$$

From the property of the angle functions as expressed by Eq. (14), the inner integral reduces the above to

$$\frac{2c}{\pi} R_{0n}^2(c,1) \int_{-T/2}^{T/2} I(t')\ S_{0n}\left(c, \frac{2t'}{T}\right) dt'\ . \tag{28}$$

Dividing both sides of Eq. (26) by $(2c/\pi)\, R_{0n}^2(c,1)$ yields

$$\frac{\pi}{2c} \int_{-T/2}^{T/2} \frac{I'(t)\ S_{0n}\left(c, \frac{2t}{T}\right)}{R_{0n}^2(c,1)}\, dt = \int_{-T/2}^{T/2} I(t')\ S_{0n}\left(c, \frac{2t'}{T}\right) dt' \tag{29}$$

Multiplying the above equation by $S_{0n}(c,x)/N_n$ and summing over all n gives

$$\frac{\pi}{2c} \sum_{n=0}^{\infty} \frac{S_{0n}(c,x)}{N_n} \int_{-T/2}^{T/2} \frac{I'(t)\ S_{0n}\left(c, \frac{2t}{T}\right)}{R_{0n}^2(c,1)}\, dt = \sum_{n=0}^{\infty} \frac{S_{0n}(c,x)}{N_n} \int_{-T/2}^{T/2} I(t')\ S_{0n}\left(c, \frac{2t'}{T}\right) dt'\ . \tag{30}$$

Interchanging the orders of integration and summation on the right yields

$$\int_{-T/2}^{T/2} I(t') \sum_{n=0}^{\infty} \frac{S_{0n}(c,x)\ S_{0n}\left(c, \frac{2t'}{T}\right)}{N_n}\, dt'\ , \tag{31}$$

which by the completeness property of Eq. (15) reduces the above to

$$\int_{-T/2}^{T/2} I(t')\ \delta\left(x - \frac{2t'}{T}\right) dt' = I\left(\frac{T}{2}x\right). \tag{32}$$

Returning to the left-hand side of Eq. (30) and defining

$$I_n = \frac{\pi}{2c} \int_{-T/2}^{T/2} \frac{I'(t)\ S_{0n}\left(c, \frac{2t}{T}\right)}{N_n R_{0n}^2(c,1)}\, dt\ , \tag{33}$$

we have the desired relationship for the object function as

$$\sum_{n=0}^{\infty} S_{0n}(c,x) I_n = I\left(\frac{T}{2}x\right)\ . \tag{34}$$

This relationship states that given a segment $|t| < T/2$ of the diffraction-limited image $I'(t)$ of some object which is known to lie entirely within the image segment, the object $I(t)$ may be reconstructed exactly. Again, for exact reconstruction the image must be noise free, and an infinite number of degrees of angle functions must be employed. It should be remembered that the range from the object to the imaging aperture, wavelength, and aperture extent are involved in ω_0 and, hence, in the constant parameter $c = \omega_0(T/2)$, which appears in all wave functions.

IMAGE ENHANCEMENT OF TWO POINT SOURCES

In the previous section it was shown that from a segment of either the far field or the diffraction-limited image in a noise-free environment, the object function can be reconstructed exactly using prolate spheroidal wave functions. To illustrate the improvement in resolution that can be obtained by this reconstruction method as opposed to the diffraction-limited (Fourier) imaging method, the reconstruction process will be applied to the equal phase and amplitude point sources considered previously.

Let the two point sources be known to exist within $|t| \leq T/2$, and in particular at $t = T/4$ and at $t = -T/4$. Then the far field from these two equal points is

$$E(\omega) = \int_{-T/2}^{T/2} \left[\delta\left(t + \frac{T}{4}\right) + \delta\left(t - \frac{T}{4}\right)\right] e^{j\omega t}\, dt$$

$$= 2 \cos \frac{T}{4}\omega. \tag{35}$$

Substitution of this far field expression into the image reconstruction parameter E_n in Eq. (24) yields

$$E_n = \frac{1}{j^n \omega_0 N_n R_{0n}(c, 1)} \int_{-\omega_0}^{\omega_0} \cos \frac{T}{4}\omega\, S_{0n}\left(c, \frac{\omega}{\omega_0}\right) d\omega. \tag{36}$$

By noting that for even values of n the angle function $S_{0n}(c, \omega/\omega_0)$ is an even function of ω/ω_0, the above integral may be evaluated at $t = T/4$ by the property in Eq. (13) as

$$\int_{-\omega_0}^{\omega_0} \cos \frac{T}{4}\omega\, S_{0n}\left(c, \frac{\omega}{\omega_0}\right) d\omega = 2j^n \omega_0 R_{0n}(c, 1)\, S_{0n}\left(c, \frac{1}{2}\right), \tag{37}$$

so that use of Eq. (37) in Eq. (36) simplifies the exact object function reconstruction equation in Eq. (25) to

$$I\left(\frac{T}{2}x\right) = 2 \sum_{n=0}^{\infty} \frac{S_{0n}\left(c, \frac{1}{2}\right) S_{0n}(c, x)}{N_n}. \tag{38}$$

But since n is even, the angle functions are also even so that Eq. (38) may be written as

$$I\left(\frac{T}{2}x\right) = \sum_{n=0}^{\infty} \frac{S_{0n}\left(c, \frac{1}{2}\right) S_{0n}(c, x)}{N_n} + \sum_{n=0}^{\infty} \frac{S_{0n}\left(c, -\frac{1}{2}\right) S_{0n}(c, x)}{N_n}, \tag{39}$$

which by the completeness property in Eq. (15) simplifies to

$$I\left(\frac{T}{2}x\right) = \delta\left(x - \frac{1}{2}\right) + \delta\left(x + \frac{1}{2}\right), \tag{40}$$

which is of course the exact object function.

The diffraction-limited image $I'(t)$ can likewise be reconstructed to the exact object function in Eq. (40). From Eq. (35) the far field from two equal point sources located at $t = T/4$ and $t = -T/4$ is $2 \cos T\omega/4$, so that the diffraction-limited image by Eq. (4) is

$$I'(t) = \frac{1}{2\pi}\int_{-\omega_0}^{\omega_0} 2 \cos \frac{T}{4}\omega e^{-j\omega t}\, d\omega$$

$$= \frac{\omega_0}{\pi}\frac{\sin \omega_0\left(t + \frac{T}{4}\right)}{\omega_0\left(t + \frac{T}{4}\right)} + \frac{\omega_0}{\pi}\frac{\sin \omega_0\left(t - \frac{T}{4}\right)}{\omega_0\left(t - \frac{T}{4}\right)}. \tag{41}$$

Substituting this expression for $I'(t)$ into the image reconstruction parameter I_n in Eq. (33) gives

$$I_n = \frac{\pi}{2c N_n R_{0n}^2(c,1)}\int_{-T/2}^{T/2}\frac{\omega_0}{\pi}\left[\frac{\sin \omega_0\left(t + \frac{T}{4}\right)}{\omega_0\left(t + \frac{T}{4}\right)} + \frac{\sin \omega_0\left(t - \frac{T}{4}\right)}{\omega_0\left(t - \frac{T}{4}\right)}\right] S_{0n}\left(c, \frac{2t}{T}\right) dt. \tag{42}$$

Using the property of these wave functions as expressed by Eq. (14) in Eq. (42) simplifies the exact object function reconstruction equation in Eq. (34) to

$$I\left(\frac{T}{2}x\right) = \sum_{n=0}^{\infty}\frac{S_{0n}\left(c, \frac{1}{2}\right) S_{0n}(c,x)}{N_n}$$

$$+ \sum_{n=0}^{\infty}\frac{S_{0n}\left(c, -\frac{1}{2}\right) S_{0n}(c,x)}{N_n}, \tag{39}$$

which again by the completeness property in Eq. (15) becomes the exact image

$$I\left(\frac{T}{2}x\right) = \delta\left(x - \frac{1}{2}\right) + \delta\left(x + \frac{1}{2}\right). \tag{40}$$

Hence, it has been illustrated by example that by using either a segment of the far field or the diffraction-limited image of two point sources, the object function may be reconstructed exactly using prolate spheroidal wave functions.

To find a value of c for which two equal points are not resolvable by Fourier imaging, consider the diffraction-limited image of two equal points as given by Eq. (41) in the $x = 2t/T$ scale:

$$I'(x) = \frac{\omega_0}{\pi}\frac{\sin c\left(x - \frac{1}{2}\right)}{c\left(x - \frac{1}{2}\right)} + \frac{\omega_0}{\pi}\frac{\sin c\left(x + \frac{1}{2}\right)}{c\left(x + \frac{1}{2}\right)} \tag{43}$$

where use has been made of the relation $c = \omega_0(T/2)$. Clearly the two points are resolved in the Rayleigh sense if $c \geq \pi$. Hence, if c is chosen to equal 2, a meaningful test of image enhancement below the classical limit of resolution can be performed.

The diffraction-limited image of two equal points is shown in Fig. 3a for $c = 2$. Assuming the object is contained within $|x| \leq 1$, the reconstructed image as given by Eq. (39) for enhancement of $n = 0$ through $n = M$ degrees, shown also in Fig. 3, where specifically M = 10 (Fig. 3b), M = 20 (Fig. 3c), and M = 40 (Fig. 3d), clearly illustrates that the two points are resolved by this process.

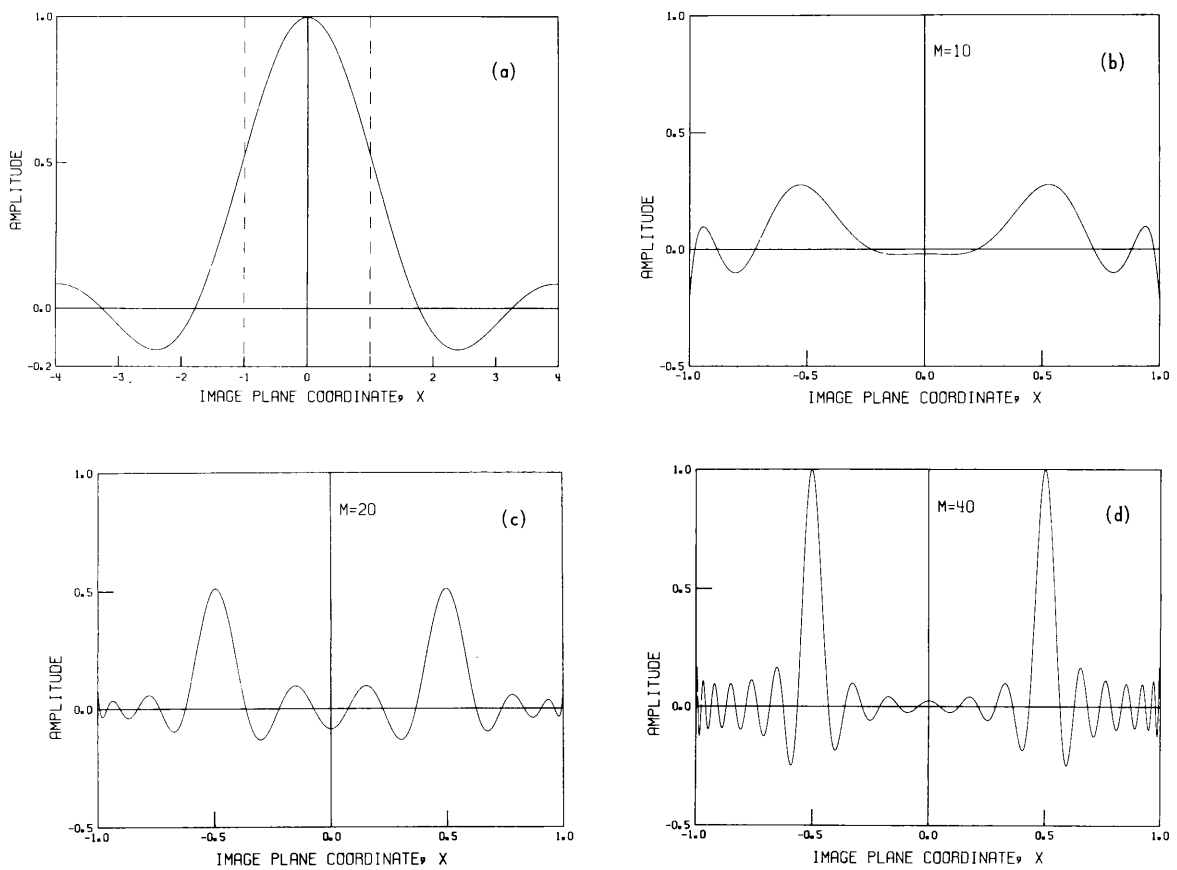

Fig. 3 - The $c = 2$ diffraction-limited image (a) and the enhanced images (b), (c), and (d) of two equal point sources for $M + 1$ degrees of enhancement

THE POINT SPREAD FUNCTION

In any real reconstruction process the number of degrees of the wave functions which are used will certainly be finite. This means that the completeness property of Eq. (15) does not hold exactly. The summation over a finite number of n values will not give a delta function but something akin to the point spread function in diffraction-limited imaging systems. However, the width of this spread function in the reconstruction process is considerably narrower than the one for the Fourier imaging process. Hence, an improvement in resolution is possible if enough wave functions are employed.

To illustrate the dependence of the point spread function of this enhancement system on the number of terms employed, consider a point source of unit amplitude located at $t = 0$, $I(t) = \delta(0)$. The far field by Eq. (3) is then $E(\omega) = 1$, so that the reconstruction parameter E_n of Eq. (24) becomes

$$E_n = \frac{1}{2j^n \omega_0 N_n R_{0n}(c, 1)} \int_{-\omega_0}^{\omega_0} S_{0n}\left(c, \frac{\omega}{\omega_0}\right) d\omega . \tag{44}$$

By the property of Eq. (13) at $t = 0$, the reconstructed image becomes

$$I\left(\frac{T}{2} x\right) = \sum_{n=0}^{M} \frac{S_{0n}(c, x) \; S_{0n}(c, 0)}{N_n} , \tag{45}$$

which is simply the completeness relation of Eq. (15) if an infinite number of the angle functions are summed. For $c = 2$ this point response function is shown up through degree M of enhancement in Fig. 4. Note that the main lobe width reduces rapidly from $M = 10$ (Fig. 4a) to $M = 20$ (Fig. 4b), but much less reduction occurs from $M = 30$ (Fig. 4c) to $M = 40$ (Fig. 4d).

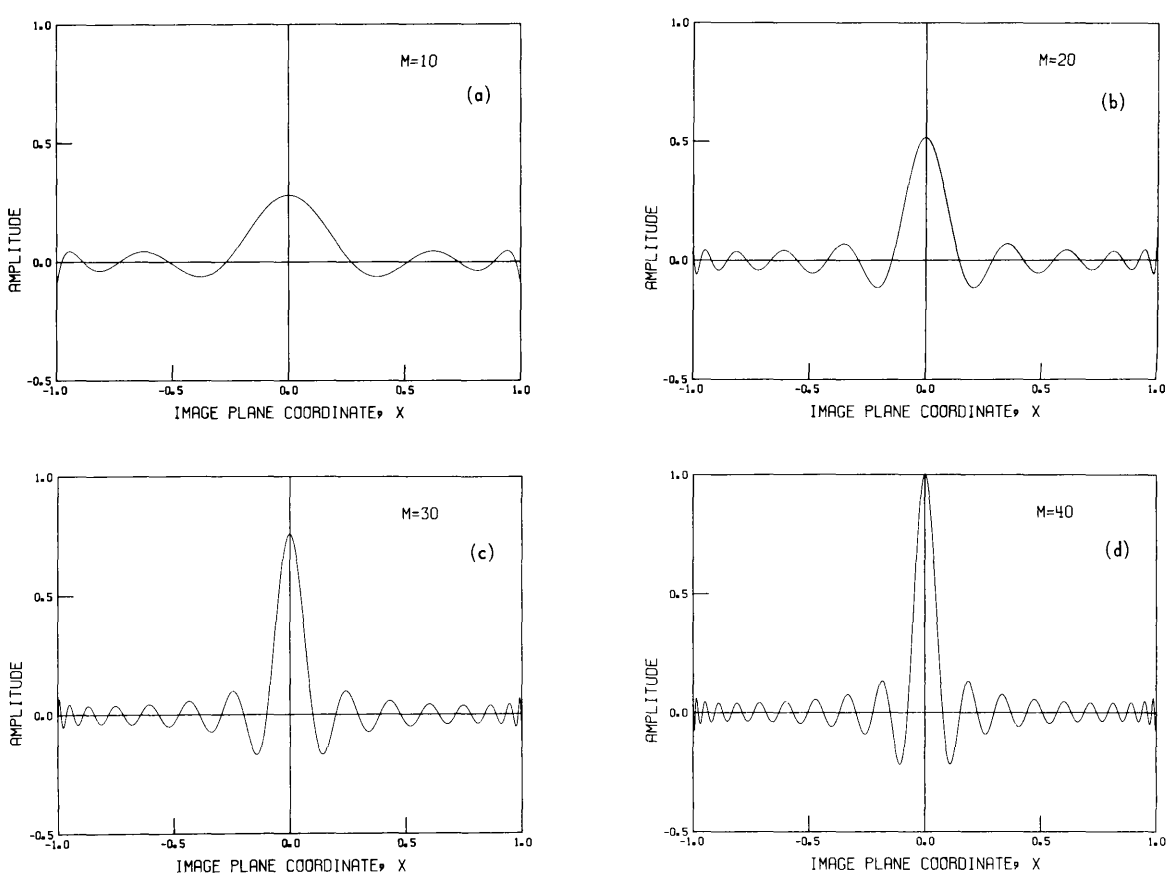

Fig. 4 - The point-response function of the $c = 2$ enhancement process for $M + 1$ degrees of enhancement

The dependence of the main lobe width on the number of degrees of enhancement $M+1$ can be more vividly illustrated by a comparison with the point response function lobe width of the $c = 2$ diffraction-limited system. For the Fourier imaging system the point response function is simply

$$I'(x) = \frac{\omega_0}{\pi} \frac{\sin 2x}{2x} . \tag{46}$$

The width of this main lobe is π. The main lobe widths of the enhanced system in Eq. (45) were measured from $M = 2$ to $M = 40$ in increments of two and divided by π to give the enhanced lobe width relative to the Fourier system lobe width. The results of these calculations are shown in Fig. 5. There is no point in the figure for $M = 0$, because the angle function $S_{00}(2,x)$ has no zeros within $|x| \leq 1$. Hence, the point response function of Eq. (45) also has no zeros by which lobe width is measured within this valid enhancement range of $|x| \leq 1$. For only $M = 2$ degrees of enhancement the main lobe width is less than half of its diffraction-limited counterpart, and for $M = 20$ the resolution has been improved over ten times that of the Rayleigh case. Above $M = 20$ the improvement is much more gradual. The failure of these points to lie precisely on a smooth curve is due to the approximation of the zeros of the main lobe by linear interpolation between adjacent values of x between which the response function changes sign.

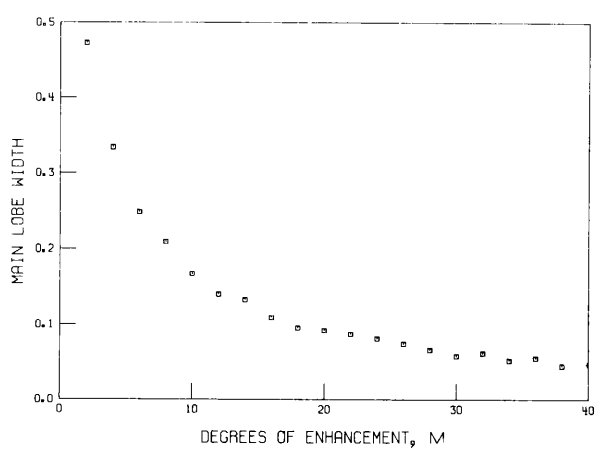

Fig. 5 - The point-response-function main lobe width of the enhancement process relative to that of the corresponding $c = 2$ Fourier imaging system for $M+1$ degrees of enhancement

GENERATION OF THE WAVE FUNCTIONS

The prolate spheroidal angle functions are generally found as a weighted summation of Legendre polynomials of the first kind with d_r^{0n} designating the weight of the rth-degree polynomial for the nth-degree, order zero angle function. There is a noticeable lack of tabulation in the literature of these d_r^{0n} expansion coefficients and of the angle functions themselves. Flammer (5), whose book is now out of print, provides the d_r^{0n} coefficients for $n = 0(1)3$* and for $c = 0(0.2)5$ and the angle functions $S_{0n}(c, \cos\theta)$ for $\theta = 0°(5°)90°$,

*This notation designates that n takes on values from 0 to 3 in steps of 1.

n = 0(1)3, and c = 0.5(0.5)5. These tables are reproduced in the readily available NBS Handbook AMS 55 (9). More extensive tabulations of the angle functions $S_{0n}(c,x)$ can be found in an AFCRL report (10) for c = 0.1(0.1)10, n = 0(1)20, and x = 0(0.05)1.

Although these tabulations provided an independent verification of the expansion coefficients and angle functions generated in this report, neither the range of the degree n nor the increment of x was sufficient for the production of the enhanced images shown in the previous section. Also, in a real situation, it may not be convenient or desirable to force the parameters of the object and aperture extents, range to the object, and wavelength to fit a predetermined value of the constant c which appears in the angle function $S_{0n}(c,x)$. Hence, it is advantageous to have the capability of generating the angle functions for any value of c and for any increment of x.

Legendre Polynomial Expansion

The procedure described in this section for determining the angle function expansion coefficients follows that of Flammer (5) but with several typographical corrections made.

Since the differential equation

$$(1-x^2)\, S''_{0n}(c,x) - 2x\, S'_{0n}(c,x) + (\lambda_{0n} - c^2x^2)\, S_{0n}(c,x) = 0\,, \tag{47}$$

which is satisfied by the angle functions, differs from the one which is satisfied by the associated Legendre functions for $c=0$ only by an essential singularity at infinity, an expansion in Legendre functions is suggested:

$$S_{0n}(c,x) = \sum_{r=0,1}^{\infty}{}' \; d_r^{0n}(c)\; P_r^0(x)\,. \tag{48}$$

Here the prime indicates a summation over either even or odd values of r, depending on whether n is even or odd. Substitution of Eq. (48) into the differential equation in Eq. (47) yields a three-term recursion formula for the d_r^{0n} coefficients:

$$A\, d_{r+2}^{0n} + (\gamma_r - \lambda_{0n})\, d_r^{0n} + B\, d_{r-2}^{0n} = 0\,. \tag{49}$$

The factors A, B, and γ_r are functions only of r and c:

$$A = \frac{(r+2)(r+1)c^2}{(2r+3)(2r+5)}\,, \tag{50a}$$

$$B = \frac{r(r-1)c^2}{(2r-3)(2r-1)}\,, \tag{50b}$$

$$\gamma_r = r(r+1) + \frac{2r^2+2r-1}{(2r-1)(2r+3)}\, c^2\,. \tag{50c}$$

By letting

$$N_r = \frac{2r-3}{2r+1}\, B\, \frac{d_r}{d_{r-2}}\,, \tag{51}$$

the ratio of d_{r+2} to d_r can be found as

$$N_{r+2} = A \frac{d_{r+2}}{d_r}$$

$$= \lambda_{0n} - \gamma_r - \frac{\beta_r}{N_r} , \tag{52}$$

where

$$\beta_r = \frac{r^2 (r-1)^2 c^4}{(2r-1)^2 (2r-3)(2r+1)} \tag{53}$$

and where the initial coefficient ratios are defined as

$$N_2 = \lambda_{0n} - \gamma_2 \tag{54a}$$

and

$$N_3 = \lambda_{0n} - \gamma_3 \tag{54b}$$

Equation (52) may be solved for the ratio of d_r to d_{r-2} for $r \geq 2$ as

$$N_r = \frac{\beta_r}{\lambda_{0n} - \gamma_r - N_{r+2}} . \tag{55}$$

From the condition that

$$\lim_{r \to \infty} N_r = 0 \tag{56}$$

the convergent infinite continued fraction expansion of Eq. (55) for $r = n$ is

$$N_{n+2} = \cfrac{\beta_n}{\lambda_{0n} - \gamma_n - \cfrac{\beta_{n+2}}{\lambda_{0n} - \gamma_{n+2} - \cfrac{\beta_{n+4}}{\lambda_{0n} - \gamma_{n+4} - \cdots}}} . \tag{57}$$

Similarly, from the condition that $d_r^{0n} = 0$ for $r < 0$, Eq. (52) may be expanded into the finite continued fraction

$$N_{n+2} = \lambda_{0n} - \gamma_n - \cfrac{\beta_n}{\lambda_{0n} - \gamma_{n-2} - \cfrac{\beta_{n-2}}{\lambda_{0n} - \gamma_{n-4} - \cdots}} . \tag{58}$$

Equating N_{n+2} in Eq. (57) as computed downward from some $N_r = 0$ to N_{n+2} in Eq. (58) as computed upward from N_2 or N_3 yields a transcendental equation, the roots of which are the eigenvalues λ_{0n}, which is of the form

$$U(\lambda_{0n}) = U_1(\lambda_{0n}) + U_2(\lambda_{0n}) = 0 , \tag{59}$$

where

$$U_1 = N_{n+2} \tag{60}$$

as computed upward from Eq. (58) and

$$U_2 = -N_{n+2} \tag{61}$$

as computed downward from Eq. (57).

A method of Bouwkamp (11), also briefly discussed by Flammer (5), provides a method whereby the transcendental equation in Eq. (59) is used to obtain a correction factor $\delta\lambda$ to an estimated value of λ. For small values of c (<10), the first estimate can be simply

$$\lambda_{0n} = n(n+1) , \tag{62}$$

which are the eigenvalues of the differential equation in Eq. (47) for $c = 0$. Writing the transcendental equation in Eq. (59) as

$$\begin{aligned} O = U &= U(\lambda + \delta\lambda) \\ &\approx U(\lambda) + \delta U \\ &\approx U_1 + U_2 + \delta U_1 + \delta U_2 \end{aligned} \tag{63}$$

and defining

$$\Delta_1 = \frac{\delta U_1}{\delta\lambda} \tag{64a}$$

and

$$\Delta_2 = \frac{\delta U_2}{\delta\lambda} , \tag{64b}$$

the correction factor $\delta\lambda$ is found to be

$$\delta\lambda = -\frac{U_1 + U_2}{\Delta_1 + \Delta_2} , \tag{65}$$

so that the corrected eigenvalue λ' is

$$\lambda' = \lambda + \delta\lambda . \tag{66}$$

The Δ_1 and Δ_2 terms in Eq. (64) can be found from the first variations of N_{r+2} and N_r with respect to λ as given by Eqs. (52) and (55) as

$$\delta N_{r+2} = \delta\lambda + \frac{\beta_r}{(N_r)^2}\,\delta N_r \tag{67a}$$

and

$$\delta N_r = -\frac{(N_r)^2}{\beta_r}\left[\delta\lambda_{0n} - \delta N_{r+2}\right] . \tag{67b}$$

Hence,

$$\begin{aligned} \Delta_1 &= \frac{\delta U_1}{\delta\lambda_{0n}} = \frac{\delta N_{n+2}}{\delta\lambda_{0n}} \\ &= \left[1 + \frac{\beta_n}{(N_n)^2}\left[1 + \frac{\beta_{n-2}}{(N_{n-2})^2}\left[1 + \frac{\beta_{n-4}}{(N_{n-4})^2}\left[\ldots,\right.\right.\right.\right. \end{aligned} \tag{68}$$

where the last term is $\beta_2/(N_2)^2$, if n is even, and $\beta_3/(N_3)^2$, if n is odd. Also

$$\Delta_2 = \frac{\delta U_2}{\delta \lambda_{0n}} = -\frac{\delta N_{n+2}}{\delta \lambda_{0n}}$$

$$= \frac{(N_{n+2})^2}{\beta_{n+2}} \left[1 + \frac{(N_{n+4})^2}{\beta_{n+4}} \left[1 + \frac{(N_{n+6})^2}{\beta_{n+6}} \left[\ldots , \right. \right. \right. \tag{69}$$

where the last term $(N_K)^2/\beta_K$ is insignificantly small.

Since the eigenvalues were accurately determined by Bouwkamp's method, the values of N_r were automatically computed so that the expansion coefficients d_r^{0n} can be computed from Eq. (51) as

$$\frac{d_r}{d_{r-2}} = \frac{4r^2 - 1}{r(r-1)c^2} N_r . \tag{70}$$

This relation easily gives d_r relative to d_0 or d_1 depending on whether n is even or odd, respectively. These initial coefficients may be obtained from the particular normalization scheme chosen, which here will be that given in Flammer (5). Requiring for n even

$$S_{0n}(c,0) = P_n(0) = \frac{(-1)^{n/2} n!}{2^n \left(\frac{n}{2}!\right)^2} \tag{71}$$

and for n odd

$$S'_{0n}(c,0) = P'_n(0) = \frac{(-1)^{(n-1)/2}(n+1)!}{2^n \left(\frac{n-1}{2}\right)! \left(\frac{n+1}{2}\right)!} , \tag{72}$$

where the prime denotes the derivative of the function, substitution of these values at $x = 0$ into the expansion in Eq. (48) yields for n even

$$\sum_{r=0}^{\infty}{}' P_r(0)\, d_r^{0n} = P_n(0) \tag{73}$$

and for n odd

$$\sum_{r=1}^{\infty}{}' P'_r(0)\, d_r^{0n} = P'_n(0) . \tag{74}$$

Explicitly, the initial coefficients are given by

$$d_0^{0n} = \frac{P_n(0)}{P_0(0) + P_2(0)\frac{d_2}{d_0} + P_4(0)\frac{d_4}{d_0} + \ldots} \tag{75}$$

and

$$d_1^{0n} = \frac{P'_n(0)}{P_1(0) + P_3(0)\frac{d_3}{d_1} + P_5(0)\frac{d_5}{d_1} + \ldots} . \tag{76}$$

A tabulation of these d_r^{0n} expansion coefficients is given in Appendix A. The eigenvalues λ_{0n} are tabulated in Appendix B.

The prolate spheroidal radial functions $R_{0n}(c, x)$ may be found in a similar fashion as the angle functions were found, but since both satisfy the same differential equation in Eq. (47), they must be proportional to one another. In the image reconstruction process only the radial function at $x = 1$ is used, and this single value is related to the initial expansion coefficients by

$$R_{0n}(c, 1) = \frac{2^n\left(\frac{n}{2}!\right)^2 d_0^{0n}}{n!} \tag{77a}$$

for n even and by

$$R_{0n}(c, 1) = \frac{2^n c\left(\frac{n-1}{2}\right)!\left(\frac{n+1}{2}\right)! d_1^{0n}}{3(n+1)!} \tag{77b}$$

for n odd. A tabulation of these radial functions at $x = 1$ is given in Appendix B.

Another term which is needed in the enhancement process is the normalization factor N_n. As introduced initially in integral form, this factor may be found more readily in terms of the d_r^{0n} expansion coefficients as

$$N_n = 2 \sum_{r=0,1}^{\infty}{}' \frac{(d_r^{0n})^2}{2r+1} . \tag{78}$$

These normalization factors are also tabulated in Appendix B.

Power Series Expansion

The angle functions which are the solutions to the differential equation in Eq. (47) may also be expressed as the simple power series

$$S_{0n}(c, x) = \sum_{r=0,1}^{\infty}{}' a_r^{0n}(c)\, x^r . \tag{79}$$

The power series coefficients a_r, of course, can be found from the d_r and Legendre polynomial coefficients, if the latter are given; this technique was used as a cross check of the method given below. However, the power series coefficients can be found directly in a manner similar to that for the d_r.

Differentiating the angle function expansion in Eq. (79) gives

$$S'_{0n}(c, x) = \sum_{r=0,1}^{\infty}{}' a_r\, r\, x^{r-1} \tag{80}$$

and again

$$S''_{0n}(c, x) = \sum_{r=0,1}^{\infty}{}' a_r\, r(r-1)\, x^{r-2}. \tag{81}$$

Substitution of the function in Eq. (79) and its first two derivatives in Eqs. (80) and (81) into the differential equation in Eq. (47) gives

$$\sum_{r=0,1}^{\infty}{}' a_r r(r-1)x^{r-2} - \sum_{r=0,1}^{\infty}{}' a_r\left[r(r+1)-\lambda_{0n}\right]x^r - c^2\sum_{r=0,1}^{\infty}{}' a_r x^{r+2} = 0 . \tag{82}$$

Adjusting the indices so that the powers of x are r only gives

$$\sum_{r=0,1}^{\infty}{}' a_{r+2}(r+1)(r+2)x^r + \sum_{r=0,1}^{\infty}{}' a_r\left[\lambda_{0n}-r(r+1)\right]x^r - c^2\sum_{r=2,3}^{\infty}{}' a_{r-2}x^r = 0. \tag{83}$$

Defining $a_i = 0$ for $i < 0$, the index of the last summation in Eq. (83) may be extended to 0, 1. Collecting all terms under a single summation then gives

$$\sum_{r=0,1}^{\infty}{}' \left\{(r+1)(r+2)a_{r+2} + \left[\lambda_{0n}-r(r+1)\right]a_r - c^2 a_{r-2}\right\}x^r = 0 , \tag{84}$$

which contains the desired recursion formula between a_{r-2}, a_r, and a_{r+2} as

$$(r+1)(r+2)a_{r+2} + \left[\lambda_{0n}-r(r+1)\right]a_r - c^2 a_{r-2} = 0 . \tag{85}$$

Defining

$$N'_{r+2} = -(r+1)(r+2)\frac{a_{r+2}}{a_r} , \tag{86a}$$

$$\gamma'_r = r(r+1) , \tag{86b}$$

and

$$\beta'_r = -c^2 r(r-1) , \tag{86c}$$

the recursion relation in Eq. (85) becomes

$$N'_r = \frac{\beta'_r}{\lambda_{0n}-\gamma'_r-N'_{r+2}} , \tag{87}$$

which is the same form as the recursion relationship in Eq. (55) for the d_r coefficients. Hence, the same method and formulas may be used for computation of the power series coefficients relative to a_0 or a_1 as was used for the Legendre expansion simply by redefining N_r, γ_r, and β_r according to Eq. (86). A tabulation of these power series expansion coefficients is given in Appendix C.

In using Eq. (87) an M is picked such that the error in the computation of N'_m without the N'_{M+2} term is less than some predetermined accuracy ϵ. Expressed in a formal way

$$\left|\frac{N''_M}{N'_M} - 1\right| < \epsilon , \tag{88}$$

where N''_M is N'_M without the N'_{M+2} term. Simplifying Eq. (88) yields

$$\left| \frac{N'_{M+2}}{\lambda_{0n} - \gamma_M} \right| < \epsilon . \tag{89}$$

If the error in the computation of N'_M without the N'_{M+2} term is negligible, then certainly the error in the N'_{M+2} term without using N'_{M+4} is also negligible, so that Eq. (89) becomes

$$\left| \frac{c^2(M+2)(M+1)}{[\lambda_{0n} - M(M+1)]\,[\lambda - (M+2)(M+3)]} \right| < \epsilon . \tag{90}$$

Now the eigenvalues λ_{0n} are on the order of $n(n+1)$, and since $n << M$, Eq. (90) can be approximated by

$$\frac{c^2}{M(M+3)} < \epsilon . \tag{91}$$

Solving for M and noting that $c >> \epsilon$,

$$M > \frac{c}{\sqrt{\epsilon}} . \tag{92}$$

For example, for $c = 2$ and a decimal accuracy of 10^{-6}, M is approximately 2000 or greater.

The initial expansion coefficients a_0 and a_1 may again be found directly from the same normalization requirement as before. For n even

$$S_{0n}(c, 0) = a_0 = P_n(0) \tag{93}$$

and for n odd

$$S'_{0n}(c, 0) = a_1 = P'_n(0) , \tag{94}$$

which is much simpler than for the d_0 and d_1 coefficients.

Another term which is required in the enhancement process is the normalization term which was defined in the integral form as

$$N_n = \int_{-1}^{1} \left[S_{0n}(c, x)\right]^2 dx . \tag{16}$$

The integrand expressed as a power series for n even is

$$\left[S_{0n}(c, x)\right]^2 = \sum_{i=0}^{\infty} b_i^{0n} x^i , \tag{95}$$

where the coefficients b_i are

$$b_i^{0n} = \sum_{j=0}^{i} a_j^{0n} a_{i-j}^{0n} . \tag{96}$$

The normalization factor is then

$$N_n = \int_{-1}^{1} \left[\sum_{i=0}^{\infty}{}' \, b_i^{0n} x^i \right] dx$$

$$= 2 \sum_{i=0}^{\infty}{}' \frac{b_i^{0n}}{i+1} \, . \tag{97}$$

The integrand expressed as a power series for n odd is

$$\left[S_{0n}(c, x) \right]^2 = \sum_{i=1}^{\infty}{}' \, b_i^{0n} x^{i+1} \, , \tag{98}$$

where

$$b_i^{0n} = \sum_{j=1}^{i}{}' \, a_j^{0n} a_{i-j}^{0n} \, , \tag{99}$$

so that the normalization factor becomes for n odd

$$N_n = 2 \sum_{i=1}^{\infty}{}' \frac{b_i^{0n}}{i+2} \, . \tag{100}$$

Verification of Results

Although care was exercised at each step of the generation of the eigenvalues and the relative and absolute expansion coefficients to reduce series truncation error to the same order as roundoff error, verification of the results is still highly desirable. The NBS Handbook (9) and the AFCRL report (10) mentioned earlier provided some substantiation of the overlapping range of values for $c = 2$.

However, by far the most useful verification was provided by W. H. Buckler of the NRL Acoustics Division who, on request, provided the author with a set of Legendre polynomial expansion coefficients at $c = 2$ for n = 0(1)36 in double precision (25 significant figures). His method of checking used the Wronskian for the angle functions of the first and second kinds and the first derivatives of each. The single-precision (10 significant figures) d_r^{0n} expansion coefficients shown in Appendix A agreed through the ninth significant figure with those provided by Buckler. By recombining Buckler's double-precision d_r^{0n} coefficients with the proper coefficients of the Legendre polynomials, a verification within eight significant figures of the single-precision power series coefficients shown in Appendix C was obtained. Such a recombination using single precision is not possible due to the rapid accumulation of roundoff error.

An indirect check of the generated angle functions can be performed by the basic differential equation in Eq. (47) at $x = 1$ which simplifies to

$$\frac{S'_{0n}(c, 1)}{S_{0n}(c, 1)} = \frac{\lambda_{0n} - c^2}{2} \, . \tag{101}$$

Again this check must be performed in double precision, because roundoff error in single precision is prohibitive in the derivative at $x = 1$. Using Buckler's data, Eq. (101) was satisfied by both the Legendre polynomial expansion and the power series expansion within one part in 10^{-25} at $n = 0$ with an almost linear decrease down to 10^{-14} at $n = 36$.

Another consideration is that of the number of expansion coefficients necessary to reduce the series truncation error to the order of roundoff. Of course the number of terms required varies both with order n and with the independent variable x. For $x = 1$ the largest number of expansion coefficients will be needed for any given n. By computing the partial sums of the angle function series expansions at $x = 1$, the number of terms necessary to reduce the truncation error to that of the same order as roundoff is readily observed. For the Legendre polynomial expansion in Eq. (48) the following empirical formula gives the necessary number of expansion coefficients for single-precision computation of the angle functions

$$\left(\frac{n}{20}\right)^2 + \frac{n}{3} + 7 , \tag{102}$$

and for the power series expansion in Eq. (79) the number of coefficients is given by

$$\left(\frac{n}{12.6}\right)^2 + \frac{n}{1.33} + 16 . \tag{103}$$

The tables of the expansion coefficients in Appendixes A and C include a sufficient number of coefficients according to the above criteria.

SUMMARY

If the electric field in the Fraunhofer region of a radiating source can be related to the source current by a Fourier transform, the inverse transformation taken over the finite limits of a known segment of the far field will produce the diffraction-limited image of the source current. This diffraction-limited image can also be formulated as the convolution of the object current with the $\sin x/x$ point spread function of the finite aperture imaging system. Both of these formulations may be solved explicitly and exactly for the object function given either the far field or the diffraction-limited image in a noise-free environment by using the special properties of prolate spheroidal wave functions. Although exact reconstruction requires an infinite number of these wave functions, considerable image enhancement and resolution improvement beyond the classical Rayleigh limit can be obtained with only ten or 20 degrees of processing. A simple example of two equal point sources unresolvable in the Rayleigh sense readily illustrates the resolution improvement capability of this process. Because of the meager tabulation of these wave functions in the literature, the method of generating the Legendre polynomial expansion coefficients and the power series expansion coefficients of these functions was given in detail with a tabulation of the results.

ACKNOWLEDGMENTS

The encouragement of Messrs. P. J. Allen and I. D. Olin for the author to pursue this investigation is appreciated. Also the assistance of W. H. Buckler of the NRL Acoustics Division in providing a set of expansion coefficients on which verification of much of the results depended is gratefully acknowledged.

REFERENCES

1. Skolnik, M.I., "Introduction to Radar Systems," New York:McGraw-Hill, p. 265, 1962

2. Silver, S., ed., "Microwave Antenna Theory and Design," MIT Radiation Lab. Series, Vol. 12, New York:McGraw-Hill, p. 169, 1949

3. Brown, H.A., "Some Basic Aspects of Radar Target Imaging," NRL Report 6623, Nov. 15, 1967

4. Bracewell, R., "The Fourier Transform and Its Applications," New York:McGraw-Hill, p. 110, 1965

5. Flammer, C., "Spheroidal Wave Functions," Stanford:Stanford University, 1957

6. Slepian, D., and Pollak, H.O., "Prolate Spheroidal Wave Functions, Fourier Analysis and Uncertainty — I," Bell System Tech. J., Vol. 40, pp. 43-63, Jan. 1961

7. Buck, G.J., and Gustincic, J.J., "Resolution Limitations of a Finite Aperture," IEEE Trans. on Antennas and Prop. AP-15(No. 3):376-381 (1967)

8. Rushforth, C.K., and Harris, R.W., "Restoration, Resolution, and Noise," J. Opt. Soc. Am. 58(No. 4):539-545 (1968)

9. Abramowitz, M., and Stegun, I.A., ed., "Handbook of Mathematical Functions with Formulas, Graphs, and Mathematical Tables," Applied Mathematics Series 55, National Bureau of Standards, Washington:U.S. Govt. Print. Off., 1966

10. Hunter, H.E., et al., "Tables of Prolate Spheroidal Functions for $m = 0$, Vol. II," AFCRL-65-283(II), Apr. 1965

11. Bouwkamp, C.J., "On Spheroidal Wave Functions of Order Zero," J. Math. Phys. 26:79-92 (1947)

This page intentionally left blank.

Appendix A

THE COEFFICIENTS OF THE PROLATE SPHEROIDAL ANGLE FUNCTION LEGENDRE POLYNOMIAL EXPANSION

d_r^{0n} = D COEFFICIENT

This page intentionally left blank.

N	R	D COEFFICIENT	N	R	D COEFFICIENT
0	0	8.31618991-001	1	1	7.92760280-001
0	2	-3.20587980-001	1	3	-1.30491677-001
0	4	2.10622161-002	1	5	5.97968297-003
0	6	-5.95512890-004	1	7	-1.30795467-004
0	8	9.38759904-006	1	9	1.68419464-006
0	10	-9.43710366-008	1	11	-1.43184143-008
0	12	6.57632997-010	1	13	8.64641366-011

N	R	D COEFFICIENT	N	R	D COEFFICIENT
2	0	8.39202240-002	3	1	6.76858005-002
2	2	1.08451884+000	3	3	9.57492177-001
2	4	-1.07998762-001	3	5	-6.79487256-002
2	6	3.65959431-003	3	7	1.81857167-003
2	8	-6.39157444-005	3	9	-2.63670709-005
2	10	6.86478544-007	3	11	2.42510649-007
2	12	-5.01050418-009	3	13	-1.54902666-009
2	14	2.65193330-011	3	15	7.29180410-012

N	R	D COEFFICIENT	N	R	D COEFFICIENT
4	0	1.44409253-003	5	1	1.09666396-003
4	2	5.61070465-002	5	3	4.41971206-002
4	4	1.02293697+000	5	5	9.81817303-001
4	6	-5.65197954-002	5	7	-4.44374947-002
4	8	1.24998160-003	5	9	8.37021714-004
4	10	-1.54895681-005	5	11	-9.05270556-006
4	12	1.24557216-007	5	13	6.46484442-008
4	14	-7.07248239-010	5	15	-3.30318141-010
4	16	2.99764062-012	5	17	1.27301647-012

N	R	D COEFFICIENT	N	R	D COEFFICIENT
6	0	1.02359929-005	7	1	7.72048334-006
6	2	8.19354403-004	7	3	6.03691285-004
6	4	3.86028640-002	7	5	3.28362251-002
6	6	1.01064294+000	7	7	9.90109234-001
6	8	-3.87401234-002	7	9	-3.29146026-002
6	10	6.35239040-004	7	11	4.77731127-004
6	12	-6.09289769-006	7	13	-4.11530792-006
6	14	3.91211199-008	7	15	2.39966118-008
6	16	-1.81653822-010	7	17	-1.02093369-010
6	18	6.41741700-013	7	19	3.32885671-013

N	R	D COEFFICIENT	N	R	D COEFFICIENT
8	0	4.03807630-008	9	1	3.03849550-008
8	2	5.50295367-006	9	3	3.88217892-006
8	4	4.75966681-004	9	5	3.74507947-004
8	6	2.94783939-002	9	7	2.60735647-002
8	8	1.00615259+000	9	9	9.93808199-001
8	10	-2.95275101-002	9	11	-2.61049811-002
8	12	3.84351563-004	9	13	3.07981193-004
8	14	-3.00420867-006	9	15	-2.20287864-006
8	16	1.60415570-008	9	17	1.08471704-008
8	18	-6.29661721-011	9	19	-3.95142533-011
8	20	1.90600664-013	9	21	1.11605634-013

N	R	D COEFFICIENT	N	R	D COEFFICIENT
10	0	1.01549165-010	11	1	7.63257226-011
10	2	2.10732071-008	11	3	1.44264147-008
10	4	2.87375818-006	11	5	2.14151483-006
10	6	3.08118748-004	11	7	2.53495357-004
10	8	2.38467090-002	11	9	2.16037429-002
10	10	1.00400980+000	11	11	9.95765368-001
10	12	-2.38681225-002	11	13	-2.16185724-002
10	14	2.57455532-004	11	15	2.14766408-004
10	16	-1.69718925-006	11	17	-1.31279069-006
10	18	7.75286610-009	11	19	5.59212105-009
10	20	-2.63446621-011	11	21	-1.78047237-011
10	22	6.97362144-014	11	23	4.43429388-014

N	R	D COEFFICIENT	N	R	D COEFFICIENT
12	0	1.76997193-013	13	1	1.32949984-013
12	2	5.19950739-011	13	3	3.48228908-011
12	4	1.02298531-008	13	5	7.32392592-009
12	6	1.65759549-006	13	7	1.29200025-006
12	8	2.15092641-004	13	9	1.82561050-004
12	10	2.00228848-002	13	11	1.84353923-002
12	12	1.00282063+000	13	13	9.96923304-001
12	14	-2.00336207-002	13	15	-1.84432574-002
12	16	1.84438040-004	13	17	1.58197855-004
12	18	-1.05089067-006	13	19	-8.44051281-007
12	20	4.19318729-009	13	21	3.16725280-009
12	22	-1.25584336-011	13	23	-8.95402892-012
12	24	2.95289843-014	13	25	1.99386610-014

N	R	D COEFFICIENT	N	R	D COEFFICIENT
14	0	2.26401017-016	15	1	1.69993518-016
14	2	8.94304377-014	15	3	5.89037936-014
14	4	2.39335915-011	15	5	1.66164347-011
14	6	5.41821385-009	15	7	4.04992032-009
14	8	1.03615519-006	15	9	8.35702105-007
14	10	1.58470488-004	15	11	1.37599635-004
14	12	1.72564566-002	15	13	1.60744022-002
14	14	1.00209223+000	15	15	9.97664244-001
14	16	-1.72624088-002	15	17	-1.60789478-002
14	18	1.38596911-004	15	19	1.21330176-004
14	20	-6.95225927-007	15	21	-5.74234166-007
14	22	2.46202951-009	15	23	1.92518268-009
14	24	-6.59058586-012	15	25	-4.89340401-012
14	26	1.39370572-014	15	27	9.85182612-015

N	R	D COEFFICIENT	N	R	D COEFFICIENT
16	0	2.21565989-019	17	1	1.66320652-019
16	2	1.13277148-016	17	3	7.36392653-017
16	4	3.95334987-014	17	5	2.67877255-014
16	6	1.18706750-011	17	7	8.58110128-012
16	8	3.10793469-009	17	9	2.40589508-009
16	10	6.88898973-007	17	11	5.70442834-007
16	12	1.21531438-004	17	13	1.07366214-004
16	14	1.51619685-002	17	15	1.42479170-002
16	16	1.00161376+000	17	17	9.98166667-001
16	18	-1.51655269-002	17	19	-1.42507224-002
16	20	1.07942618-004	17	21	9.59821674-005
16	22	-4.83545598-007	17	23	-4.08126051-007
16	24	1.53907279-009	17	25	1.23640047-009
16	26	-3.72394005-012	17	27	-2.85431531-012
16	28	7.15411389-015	17	29	5.24329783-015

N	R	D COEFFICIENT	N	R	D COEFFICIENT
18	0	1.71245784-022	19	1	1.28524470=022
18	2	1.10026359-019	19	3	7.07746369=020
18	4	4.85076958-017	19	5	3.22268540=017
18	6	1.86116998=014	19	7	1.30915145=014
18	8	6.35596632=012	19	9	4.75699255=012
18	10	1.90197048-009	19	11	1.51431364=009
18	12	4.80524613-007	19	13	4.06236169=007
18	14	9.61276220-005	19	15	8.60825365=005
18	16	1.35210554-002	19	17	1.27932883=002
18	18	1.00128259+000	19	19	9.98522909=001
18	20	=1.35233106=002	19	21	=1.27951115=002
18	22	8.64379106=005	19	23	7.78142094=005
18	24	=3.49769125-007	19	25	=3.00344540=007
18	26	1.01086070=009	19	27	8.29827073=010
18	28	=2.23120975=012	19	29	=1.75458041=012
18	30	3.92661442-015	19	31	2.96336687=015

N	R	D COEFFICIENT	N	R	D COEFFICIENT
20	0	1.07171472-025	21	1	8.04246673=026
20	2	8.45319785-023	21	3	5.39048880=023
20	4	4.59218874=020	21	5	3.00153053=020
20	6	2.18880042=017	21	7	1.50499323=017
20	8	9.41837595=015	21	9	6.85268473=015
20	10	3.63259143=012	21	11	2.79828049=012
20	12	1.22632352=009	21	13	9.98892283=010
20	14	3.48203132=007	21	15	2.99330843=007
20	16	7.79199227=005	21	17	7.05424743=005
20	18	1.22007402=002	21	19	1.16076537=002
20	20	1.00104389+000	21	21	9.98784610=001
20	22	=1.22022375=002	21	23	=1.16088891=002
20	24	7.07730614=005	21	25	6.43518771=005
20	26	=2.61115395=007	21	27	=2.27389706=007
20	28	6.91025028=010	21	29	5.77421327=010
20	30	=1.40209969-012	21	31	=1.12610958=012
20	32	2.27627775-015	21	33	1.75998384=015

N	R	D COEFFICIENT	N	R	D COEFFICIENT
22	0	5.54177835-029	23	1	4.15831583-029
22	2	5.26471002-026	23	3	3.33290115-026
22	4	3.45430217-023	23	5	2.22702715-023
22	6	2.00045174-020	23	7	1.34929544-020
22	8	1.05663933-017	23	9	7.50569187-018
22	10	5.08252684-015	23	11	3.80646371-015
22	12	2.19181251-012	23	13	1.72936179-012
22	14	8.25082065-010	23	15	6.84800515-010
22	16	2.60248633-007	23	17	2.26812826-007
22	18	6.44297787-005	23	19	5.88542184-005
22	20	1.11154077-002	23	21	1.06228256-002
22	22	1.00086616+000	23	23	9.98982478-001
22	24	-1.11164404-002	23	25	-1.06236921-002
22	26	5.90101639-005	23	27	5.41010287-005
22	28	-2.00057073-007	23	29	-1.76263212-007
22	30	4.88251710-010	23	31	4.14069388-010
22	32	-9.16610248-013	23	33	-7.49325294-013
22	34	1.38100438-015	23	35	1.08973722-015

N	R	D COEFFICIENT	N	R	D COEFFICIENT
24	0	2.40748593-032	25	1	1.80634223-032
24	2	2.71143857-029	25	3	1.70594377-029
24	4	2.11356389-026	25	5	1.34679111-026
24	6	1.46075926-023	25	7	9.69181777-024
24	8	9.27887900-021	25	9	6.45646850-021
24	10	5.42992641-018	25	11	3.96892648-018
24	12	2.89747490-015	25	13	2.22391709-015
24	14	1.38366041-012	25	15	1.11388902-012
24	16	5.75036230-010	25	17	4.84814969-010
24	18	1.99550937-007	25	19	1.75918491-007
24	20	5.41593644-005	25	21	4.98441234-005
24	22	1.02074405-002	25	23	9.79183682-003
24	24	1.00073026+000	25	25	9.99135696-001
24	26	-1.02081755-002	25	27	-9.79246231-003
24	28	4.99532634-005	25	29	4.61163989-005
24	30	-1.56641445-007	25	31	-1.39378050-007
24	32	3.54687491-010	25	33	3.04596498-010
24	34	-6.19527338-013	25	35	-5.14138218-013
24	36	8.70710803-016	25	37	6.99105007-016

N	R	D COEFFICIENT	N	R	D COEFFICIENT
26	0	8.91033035-036	27	1	6.68505457=036
26	2	1.17393841-032	27	3	7.34688789=033
26	4	1.07224508-029	27	5	6.76387442=030
26	6	8.71398161-027	27	7	5.69963741=027
26	8	6.54703584-024	27	9	4.47455288=024
26	10	4.57141612-021	27	11	3.27125652=021
26	12	2.94715449-018	27	13	2.20808402=018
26	14	1.73070542-015	27	15	1.35645563=015
26	16	9.07382056-013	27	17	7.43029865=013
26	18	4.12804588=010	27	19	3.52693002=010
26	20	1.56332415-007	27	21	1.39163440=007
26	22	4.61607892=005	27	23	4.27532143=005
26	24	9.43663746=003	27	25	9.08129108=003
26	26	1.00062401+000	27	27	9.99256750=001
26	28	=9.43717469=003	27	29	=9.08175380=003
26	30	4.28318272-005	27	31	3.97763891=005
26	32	=1.24930450-007	27	33	=1.12103113=007
26	34	2.63824717=010	27	35	2.29019426=010
26	36	=4.30823750=013	27	37	=3.62195835=013
26	38	5.67371378=016	27	39	4.62428627=016

N	R	D COEFFICIENT	N	R	D COEFFICIENT
28	0	2.84319698-039	29	1	2.13303523=039
28	2	4.33232797-036	29	3	2.69882640=036
28	4	4.58251698=033	29	5	2.86539759=033
28	6	4.32483734=030	29	7	2.79370565=030
28	8	3.79093031=027	29	9	2.55041133=027
28	10	3.10916487-024	29	11	2.18371581=024
28	12	2.37690529=021	29	13	1.74328881=021
28	14	1.67704161-018	29	15	1.28361952=018
28	16	1.07582787=015	29	17	8.58476279=016
28	18	6.14643190=013	29	19	5.10723731=013
28	20	3.03895228-010	29	21	2.62617357=010
28	22	1.24734513=007	29	23	1.11964759=007
28	24	3.98106852=005	29	25	3.70732336=005
28	26	8.77409492=003	29	27	8.46679693=003
28	28	1.00053939+000	29	29	9.99354050=001
28	30	=8.77449664=003	29	31	=8.46714654=003
28	32	3.71312635-005	29	33	3.46586925=005
28	34	=1.01231521=007	29	35	=9.15026235=008
28	36	2.00279952-010	29	37	1.75490489=010
28	38	=3.07061402-013	29	39	=2.61073000=013
28	40	3.80419421-016	29	41	3.14134064=016

N	R	D COEFFICIENT	N	R	D COEFFICIENT
30	0	7.90233661-043	31	1	5.92830194-043
30	2	1.37895933-039	31	3	8.55553648-040
30	4	1.67215975-036	31	5	1.03752553-036
30	6	1.81326603-033	31	7	1.15848778-033
30	8	1.83299258-030	31	9	1.21611074-030
30	10	1.74306991-027	31	11	1.20412448-027
30	12	1.55653936-024	31	13	1.12017801-024
30	14	1.29577489-021	31	15	9.71070821-022
30	16	9.94179685-019	31	17	7.75212015-019
30	18	6.92114112-016	31	19	5.60949291-016
30	20	4.28113078-013	31	21	3.60260627-013
30	22	2.28615739-010	31	23	1.99522158-010
30	24	1.01103207-007	31	25	9.14107055-008
30	26	3.46855655-005	31	27	3.24535371-005
30	28	8.19849813-003	31	29	7.93012700-003
30	30	1.00047088+000	31	31	9.99433427-001
30	32	-8.19880448-003	31	33	-7.93039603-003
30	34	3.24972884-005	31	35	3.04682878-005
30	36	-8.31662049-008	31	37	-7.56542359-008
30	38	1.54764263-010	31	39	1.36723351-010
30	40	-2.23604366-013	31	41	-1.92005050-013
30	42	2.61521302-016	31	43	2.18449809-016

N	R	D COEFFICIENT	N	R	D COEFFICIENT
32	0	1.93025913-046	33	1	1.44802815-046
32	2	3.82432933-043	33	3	2.36426984-043
32	4	5.26992382-040	33	5	3.24748987-040
32	6	6.50590887-037	33	7	4.11612885-037
32	8	7.50987808-034	33	9	4.92099020-034
32	10	8.19021424-031	33	11	5.57473557-031
32	12	8.43758548-028	33	13	5.97003590-028
32	14	8.16750614-025	33	15	6.00597987-025
32	16	7.36313768-022	33	17	5.62347063-022
32	18	6.10753807-019	33	19	4.84031719-019
32	20	4.58741657-016	33	21	3.76894492-016
32	22	3.05494343-013	33	23	2.59933692-013
32	24	1.75250576-010	33	25	1.54273481-010
32	26	8.30797863-008	33	27	7.55915465-008
32	28	3.04896183-005	33	29	2.86459296-005
32	30	7.69378376-003	33	31	7.45738802-003
32	32	1.00041465+000	33	33	9.99499025-001
32	34	-7.69402144-003	33	35	-7.45759840-003
32	36	2.86795283-005	33	37	2.69940453-005
32	38	-6.91553784-008	33	39	-6.32633650-008
32	40	1.21473448-010	33	41	1.08092147-010
32	42	-1.65940020-013	33	43	-1.43742465-013
32	44	1.83790417-016	33	45	1.55093421-016

N	R	D COEFFICIENT	N	R	D COEFFICIENT
34	0	4.17630506-050	35	1	3.13287052-050
34	2	9.32360764-047	35	3	5.74568816-047
34	4	1.44877165-043	35	5	8.87332422-044
34	6	2.01990496-040	35	7	1.26680785-040
34	8	2.63973536-037	35	9	1.71058238-037
34	10	3.27091943-034	35	11	2.19696032-034
34	12	3.84703078-031	35	13	2.68070488-031
34	14	4.27833899-028	35	15	3.09276572-028
34	16	4.46791141-025	35	17	3.34887807-025
34	18	4.33944939-022	35	19	3.36997837-022
34	20	3.87110077-019	35	21	3.11208922-019
34	22	3.12106879-016	35	23	2.59509952-016
34	24	2.22665736-013	35	25	1.91311665-013
34	26	1.36576830-010	35	27	1.21146746-010
34	28	6.90957307-008	35	29	6.32196135-008
34	30	2.70111777-005	35	31	2.54707610-005
34	32	7.24761633-003	35	33	7.03780579-003
34	34	1.00036792+000	35	35	9.99553858-001
34	36	-7.24780354-003	35	37	-7.03797266-003
34	38	2.54969837-005	35	39	2.40816560-005
34	40	-5.81226156-008	35	41	-5.34365072-008
34	42	9.66708986-011	35	43	8.65770766-011
34	44	-1.25231187-013	35	45	-1.09328819-013
34	46	1.31718213-016	35	47	1.12167560-016

N	R	D COEFFICIENT	N	R	D COEFFICIENT
36	0	8.05935461-054	37	1	6.04562363-054
36	2	2.01383237-050	37	3	1.23748940-050
36	4	3.50457095-047	37	5	2.13469387-047
36	6	5.47917123-044	37	7	3.40936864-044
36	8	8.04623396-041	37	9	5.16196252-041
36	10	1.12365029-037	37	11	7.45698605-038
36	12	1.49532176-034	37	13	1.02766278-034
36	14	1.89134668-031	37	15	1.34620576-031
36	16	2.26134817-028	37	17	1.66633480-028
36	18	2.53606767-025	37	19	1.93345682-025
36	20	2.64119326-022	37	21	2.08172917-022
36	22	2.52216404-019	37	23	2.05350359-019
36	24	2.17293904-016	37	25	1.82602917-016
36	26	1.65360034-013	37	27	1.43307941-013
36	28	1.08000545-010	37	29	9.64480850-011
36	30	5.80805445-008	37	31	5.34053428-008
36	32	2.40955657-005	37	33	2.27954178-005
36	34	6.85036599-003	37	35	6.66289693-003
36	36	1.00032867+000	37	37	9.99600159-001
36	38	-6.85051544-003	37	39	-6.66303099-003
36	40	2.28161788-005	37	41	2.16162268-005
36	42	-4.93169769-008	37	43	-4.55434665-008
36	44	7.78870989-011	37	45	7.01576452-011
36	46	-9.59372264-014	37	47	-8.43428279-014
36	48	9.60682985-017	37	49	8.24802890-017

N	R	D COEFFICIENT	N	R	D COEFFICIENT
38	0	1.39581574-057	39	1	1.04703441-057
38	2	3.88036951-054	39	3	2.37833964-054
38	4	7.51675935-051	39	5	4.55593534-051
38	6	1.30955905-047	39	7	8.09076251-048
38	8	2.14672334-044	39	9	1.36472361-044
38	10	3.35477514-041	39	11	2.20219023-041
38	12	5.01244925-038	39	13	3.40173948-038
38	14	7.14863005-035	39	15	5.01683462-035
38	16	9.68977049-032	39	17	7.03001237-032
38	18	1.24047070-028	39	19	9.29893585-029
38	20	1.48763237-025	39	21	1.15148357-025
38	22	1.65424019-022	39	23	1.32117224-022
38	24	1.68400236-019	39	25	1.38667434-019
38	26	1.54412835-016	39	27	1.30995625-016
38	28	1.24862810-013	39	29	1.09049350-013
38	30	8.65186465-011	39	31	7.77318271-011
38	32	4.92867260-008	39	33	4.55208599-008
38	34	2.16276320-005	39	35	2.05202904-005
38	36	6.49440521-003	39	37	6.32589111-003
38	38	1.00029539+000	39	39	9.99639610-001
38	40	-6.49452596-003	39	41	-6.32600003-003
38	42	2.05369384-005	39	43	1.95107913-005
38	44	-4.22037415-008	39	45	-3.91311125-008
38	46	6.34515151-011	39	47	5.74520141-011
38	48	-7.44930877-014	39	49	-6.59049267-014
38	50	7.11810490-017	39	51	6.15657724-017

N	R	D COEFFICIENT
40	0	2.18166353-061
40	2	6.71134493-058
40	4	1.43924769-054
40	6	2.77842308-051
40	8	5.05433491-048
40	10	8.78372073-045
40	12	1.46353315-041
40	14	2.33596264-038
40	16	3.55963595-035
40	18	5.15204228-032
40	20	7.03490855-029
40	22	8.98662888-026
40	24	1.06292904-022
40	26	1.14923765-019
40	28	1.11755254-016
40	30	9.56974414-014
40	32	7.01197280-011
40	34	4.21816116-008
40	36	1.95202279-005
40	38	6.17361403-003
40	40	1.00026691+000
40	42	-6.17371265-003
40	44	1.85828938-005
40	46	-3.63951290-008
40	48	5.22103633-011
40	50	-5.85511050-014
40	52	5.34990750-017

Appendix B

THE PROLATE SPHEROIDAL EIGENVALUES AND NORMALIZATION CONSTANTS

λ_{0n} = EIGENVALUE

N_n = NORMALIZATION CONSTANT

This page intentionally left blank.

N	EIGENVALUE	NORM. CONSTANT
0	1.12773406+000	1.42438959+000
1	4.28712854+000	4.23850910-001
2	8.22571300+000	4.87151652-001
3	1.41002039+001	2.65834509-001
4	2.20548298+001	2.34288356-001
5	3.20352631+001	1.76088681-001
6	4.40247476+001	1.57646355-001
7	5.80183708+001	1.31019042-001
8	7.40141944+001	1.19315967-001
9	9.20113044+001	1.04113591-001
10	1.12009219+002	9.61158943-002
11	1.34007664+002	8.63053829-002
12	1.58006473+002	8.05178068-002
13	1.84005541+002	7.36704721-002
14	2.12004797+002	6.92962895-002
15	2.42004193+002	6.42490086-002
16	2.74003697+002	6.08301135-002
17	3.08003284+002	5.69570383-002
18	3.44002937+002	5.42128035-002
19	3.82002642+002	5.11476345-002
20	4.22002390+002	4.88970483-002
21	4.64002172+002	4.64112819-002
22	5.08001982+002	4.45325406-002
23	5.54001817+002	4.24763127-002
24	6.02001671+002	4.08845243-002
25	6.52001542+002	3.91554942-002
26	7.04001428+002	3.77897190-002
27	7.58001325+002	3.63156320-002
28	8.14001234+002	3.51310108-002
29	8.72001151+002	3.38594089-002
30	9.32001077+002	3.28221969-002
31	9.94001010+002	3.17140782-002
32	1.05800095+003	3.07984098-002
33	1.12400089+003	2.98241770-002
34	1.19200084+003	2.90098956-002
35	1.26200079+003	2.81466844-002
36	1.33400075+003	2.74178520-002
37	1.40800071+003	2.66477206-002
38	1.48400068+003	2.59915701-002
39	1.56200064+003	2.53002428-002
40	1.64200061+003	2.47064275-002

This page intentionally left blank.

Appendix C

THE COEFFICIENTS OF THE PROLATE SPHEROIDAL ANGLE FUNCTION POWER SERIES EXPANSION

d_r^{0n} = A COEFFICIENT

This page intentionally left blank.

N	R	A COEFFICIENT	N	R	A COEFFICIENT
0	0	1.00000000+000	1	1	1.00000000+000
0	2	-5.63867032-001	1	3	-3.81188091-001
0	4	1.04390822-001	1	5	5.29972628-002
0	6	-9.51255909-003	1	7	-3.85810849-003
0	8	5.13632926-004	1	9	1.73266429-004
0	10	-1.83100777-005	1	11	-5.28427984-006
0	12	4.62667093-007	1	13	1.16635671-007
0	14	-8.71433898-009	1	15	-1.94980686-009
0	16	1.27019352-010	1	17	2.55445203-011

N	R	A COEFFICIENT	N	R	A COEFFICIENT
2	0	-5.00000000-001	3	1	-1.50000000+000
2	2	2.05642825+000	3	3	3.02505097+000
2	4	-5.48084924-001	3	5	-6.17661189-001
2	6	5.90801267-002	3	7	5.42742120-002
2	8	-3.51697396-003	3	9	-2.73008800-003
2	10	1.33644450-004	3	11	8.98520510-005
2	12	-3.53278222-006	3	13	-2.09495829-006
2	14	6.88100248-008	3	15	3.65006416-008
2	16	-1.02931330-009	3	17	-4.93917870-010
2	18	1.22016950-011	3	19	5.34514802-012

N	R	A COEFFICIENT	N	R	A COEFFICIENT
4	0	3.75000000-001	5	1	1.87500000+000
4	2	-4.13528058+000	5	3	-9.38601972+000
4	4	5.65760215+000	5	5	9.77756872+000
4	6	-9.38884388-001	5	7	-1.36771437+000
4	8	6.97178508-002	5	9	8.79633303-002
4	10	-3.03852920-003	5	11	-3.38260175-003
4	12	8.82381488-005	5	13	8.79001763-005
4	14	-1.84089524-006	5	15	-1.65942945-006
4	16	2.90217703-008	5	17	2.38893236-008
4	18	-3.58593653-010	5	19	-2.71595173-010
4	20	3.57045797-012	5	21	2.50417013-012

N	R	A COEFFICIENT	N	R	A COEFFICIENT
6	0	-3.12500000-001	7	1	-2.18750000+000
6	2	6.87886682+000	7	3	2.04233643+001
6	4	-2.19014312+001	7	5	-4.74299977+001
6	6	1.84563942+001	7	7	3.35858266+001
6	8	-2.23170117+000	7	9	-3.57650892+000
6	10	1.26590815-001	7	11	1.81461132-001
6	12	-4.35563430-003	7	13	-5.64900960-003
6	14	1.02417632-004	7	15	1.21291013-004
6	16	-1.76569391-006	7	17	-1.92390533-006
6	18	2.33873512-008	7	19	2.35990472-008
6	20	-2.46220478-010	7	21	-2.31337230-010
6	22	2.11384888-012	7	23	1.85809829-012

N	R	A COEFFICIENT	N	R	A COEFFICIENT
8	0	2.73437500-001	9	1	2.46093750+000
8	2	-1.01191281+001	9	3	-3.69186991+001
8	4	5.74448415+001	9	5	1.48187851+002
8	6	-1.04777112+002	9	7	-2.22309446+002
8	8	6.40023962+001	9	9	1.19422285+002
8	10	-6.08913015+000	9	11	-1.02675668+001
8	12	2.79449475-001	9	13	4.30144462-001
8	14	-7.94302346-003	9	15	-1.12482299-002
8	16	1.56914401-004	9	17	2.05760936-004
8	18	-2.30480320-006	9	19	-2.81405091-006
8	20	2.63238457-008	9	21	3.00687951-008
8	22	-2.41419526-010	9	23	-2.59069864-010
8	24	1.82169274-012	9	25	1.84328586-012

N	R	A COEFFICIENT	N	R	A COEFFICIENT
10	0	-2.46093750-001	11	1	-2.70703125+000
10	2	1.37823844+001	11	3	5.95581454+001
10	4	-1.21837015+002	11	5	-3.63868917+002
10	6	3.75508607+002	11	7	9.06747352+002
10	8	-4.78150222+002	11	9	-1.00262109+003
10	10	2.29249461+002	11	11	4.34090927+002
10	12	-1.79788888+001	11	13	-3.12948286+001
10	14	6.92815878-001	11	15	1.11643710+000
10	16	-1.67749433-002	11	17	-2.51674192-002
10	18	2.85709935-004	11	19	4.01009400-004
10	20	-3.65558447-006	11	21	-4.82008964-006
10	22	3.66957241-008	11	23	4.56228079-008
10	24	-2.98117579-010	11	25	-3.50624233-010
10	26	2.00656347-012	11	27	2.23905231-012

N	R	A COEFFICIENT	N	R	A COEFFICIENT
12	0	2.25585938-001	13	1	2.93261719+000
12	2	-1.78220192+001	13	3	-8.89587628+001
12	4	2.25830386+002	13	5	7.65656529+002
12	6	-1.04124478+003	13	7	-2.81598054+003
12	8	2.17311528+003	13	9	5.04894081+003
12	10	-2.12296623+003	13	11	-4.41720303+003
12	12	8.37943811+002	13	13	1.60201792+003
12	14	-5.58965764+001	13	15	-9.94367823+001
12	16	1.85631298+000	13	17	3.08883386+000
12	18	-3.91458902-002	13	19	-6.11886330-002
12	20	5.85951404-004	13	21	8.63577193-004
12	22	-6.64087855-006	13	23	-9.25861078-006
12	24	5.94617257-008	13	25	7.86521749-008
12	26	-4.33563606-010	13	27	-5.45534767-010
12	28	2.63374055-012	13	29	3.15989606-012

N	R	A COEFFICIENT	N	R	A COEFFICIENT
14	0	-2.09472656-001	15	1	-3.14208984+000
14	2	2.22046039+001	15	3	1.25685790+002
14	4	-3.81257734+002	15	5	-1.44604135+003
14	6	2.44307107+003	15	7	7.31118030+003
14	8	-7.44390769+003	15	9	-1.89679772+004
14	10	1.16883896+004	15	11	2.64768799+004
14	12	-9.25795512+003	15	13	-1.91566649+004
14	14	3.10572709+003	15	15	5.97803685+003
14	16	-1.80242047+002	15	17	-3.25763970+002
14	18	5.25898715+000	15	19	8.96087512+000
14	20	-9.82239078-002	15	21	-1.58315921-001
14	22	1.31135694-003	15	23	2.00526020-003
14	24	-1.33387345-005	15	25	-1.94023853-005
14	26	1.07788818-007	15	27	1.49499949-007
14	28	-7.12876428-010	15	29	-9.44820176-010
14	30	3.94578495-012	15	31	5.00719138-012

N	R	A COEFFICIENT	N	R	A COEFFICIENT
16	0	1.96383615-001	17	1	3.33847046+000
16	2	-2.69045073+001	17	3	-1.70263821+002
16	4	6.00940079+002	17	5	2.52060020+003
16	6	-5.09162912+003	17	7	-1.67003855+004
16	8	2.11371526+004	17	9	5.85921442+004
16	10	-4.76683276+004	17	11	-1.16728013+005
16	12	5.98661407+004	17	13	1.33197963+005
16	14	-3.98631826+004	17	15	-8.21442514+004
16	16	1.16285651+004	17	17	2.24958483+004
16	18	-5.97231542+002	17	19	-1.09252217+003
16	20	1.55387462+001	17	21	2.69652016+001
16	22	-2.60447329-001	17	23	-4.29913435-001
16	24	3.13798457-003	17	25	4.93890051-003
16	26	-2.89506882-005	17	27	-4.35412876-005
16	28	2.13162380-007	17	29	3.06955934-007
16	30	-1.28986253-009	17	31	-1.78163809-009
16	32	6.55692285-012	17	33	8.70183211-012

N	R	A COEFFICIENT	N	R	A COEFFICIENT
18	0	-1.85470581-001	19	1	-3.52394104+000
18	2	3.19012123+001	19	3	2.23184484+002
18	4	-8.98620444+002	19	5	-4.12964723+003
18	6	9.70944227+003	19	7	3.46318922+004
18	8	-5.24263315+004	19	9	-1.57036208+005
18	10	1.38877266+005	19	11	4.18122865+005
18	12	-2.83238273+005	19	13	-6.74102345+005
18	14	2.96072178+005	19	15	6.49974959+005
18	16	-1.70031227+005	19	17	-3.49244746+005
18	18	4.38792040+004	19	19	8.52146878+004
18	20	-2.02108470+003	19	21	-3.73246072+003
18	22	4.74465682+001	19	23	8.35410184+001
18	24	-7.21257432-001	19	25	-1.21348411+000
18	26	7.91757443-003	19	27	1.27543274-002
18	28	-6.68327206-005	19	29	-1.03265626-004
18	30	4.57931685-007	19	31	6.70921736-007
18	32	-2.52328736-009	19	33	-3.60039407-009
18	34	1.16452228-011	19	35	1.63065913-011

N	R	A COEFFICIENT	N	R	A COEFFICIENT
20	0	1.76197052-001	21	1	3.70013809+000
20	2	-3.71777885+001	21	3	-2.84911972+002
20	4	1.28889614+003	21	5	6.43978154+003
20	6	-1.72762679+004	21	7	-6.65718767+004
20	8	1.17324619+005	21	9	3.77600408+005
20	10	-4.57033357+005	21	11	-1.28626964+006
20	12	1.08382423+006	21	13	2.74714560+006
20	14	-1.59410971+006	21	15	-3.71355288+006
20	16	1.42620986+006	21	17	3.09864887+006
20	18	-7.19971651+005	21	19	-1.47499258+006
20	20	1.66290242+005	21	21	3.24517083+005
20	22	-6.95555229+003	21	23	-1.29440893+004
20	24	1.48752165+002	21	25	2.65027639+002
20	26	-2.06873732+000	21	27	-3.53531622+000
20	28	2.08560248-002	21	29	3.42437147-002
20	30	-1.62240708-004	21	31	-2.56334470-004
20	32	1.01432176-006	21	33	1.54433289-006
20	34	-5.24533333-009	21	35	-7.70604283-009
20	36	2.29234576-011	21	37	3.25361902-011

N	R	A COEFFICIENT	N	R	A COEFFICIENT
22	0	-1.68188095-001	23	1	-3.86832619+000
22	2	4.27199428+001	23	3	3.55887180+002
22	4	-1.78718073+003	23	5	-9.64534858+003
22	6	2.90772873+004	23	7	1.20371517+005
22	8	-2.42093254+005	23	9	-8.33108551+005
22	10	1.17410497+006	23	11	3.51659425+006
22	12	-3.54745818+006	23	13	-9.53965127+006
22	14	6.88686117+006	23	15	1.69659142+007
22	16	-8.61036713+006	23	17	-1.97260532+007
22	18	6.73075541+006	23	19	1.45028090+007
22	20	-3.03094792+006	23	21	-6.19623650+006
22	22	6.35611355+005	23	23	1.24125741+006
22	24	-2.42686128+004	23	25	-4.54495260+004
22	26	4.76586380+002	23	27	8.57489607+002
22	28	-6.10796707+000	23	29	-1.05748290+001
22	30	5.69305252-002	23	31	9.49802934-002
22	32	-4.10644825-004	23	33	-6.61098535-004
22	34	2.38733562-006	23	35	3.71294682-006
22	36	-1.15068397-008	23	37	-1.73126552-008
22	38	4.69995655-011	23	39	6.84571979-011

N	R	A COEFFICIENT	N	R	A COEFFICIENT
24	0	1.61198258-001	25	1	4.02950644+000
24	2	-4.85153923+001	25	3	-4.36530900+002
24	4	2.40965830+003	25	5	1.39698284+004
24	6	-4.67539739+004	25	7	-2.06928593+005
24	8	4.67713252+005	25	9	1.71368944+006
24	10	-2.75639801+006	25	11	-8.76294386+006
24	12	1.02880552+007	25	13	2.92538402+007
24	14	-2.52720625+007	25	15	-6.56400085+007
24	16	4.14493457+007	25	17	9.98558827+007
24	18	-4.50398548+007	25	19	-1.01791957+008
24	20	3.12470918+007	25	21	6.68737927+007
24	22	-1.26994509+007	25	23	-2.59155960+007
24	24	2.43506680+006	25	25	4.76515788+006
24	26	-8.56492400+004	25	27	-1.61253629+005
24	28	1.55487609+003	25	29	2.82081621+003
24	30	-1.84775772+001	25	31	-3.23450893+001
24	32	1.60138232-001	25	33	2.70818509-001
24	34	-1.07684380-003	25	35	-1.76140823-003
24	36	5.84966101-006	25	37	9.26467495-006
24	38	-2.64099875-008	25	39	-4.05413539-008
24	40	1.01227418-010	25	41	1.50739617-010

N	R	A COEFFICIENT	N	R	A COEFFICIENT
26	0	-1.54981017-001	27	1	-4.18448746+000
26	2	5.45534286+001	27	3	5.27246345+002
26	4	-3.17324925+003	27	5	-1.96671605+004
26	6	7.23575077+004	27	7	3.40948283+005
26	8	-8.55597614+005	27	9	-3.32534466+006
26	10	6.01142604+006	27	11	2.02063494+007
26	12	-2.70774094+007	27	13	-8.11698902+007
26	14	8.16621137+007	27	15	2.23022808+008
26	16	-1.68539627+008	27	17	-4.25922021+008
26	18	2.39006561+008	27	19	5.65524589+008
26	20	-2.29460197+008	27	21	-5.13030315+008
26	22	1.43125484+008	27	23	3.04584489+008
26	24	-5.30068968+007	27	25	-1.07994683+008
26	26	9.36101979+006	27	27	1.83503254+007
26	28	-3.05270304+005	27	29	-5.77222295+005
26	30	5.15149655+003	27	31	9.41201038+003
26	32	-5.70668865+001	27	33	-1.00843964+002
26	34	4.62142263-001	27	35	7.90733118-001
26	36	-2.91036988-003	27	37	-4.82643451-003
26	38	1.48370687-005	27	39	2.38710576-005
26	40	-6.29879904-008	27	41	-9.84033191-008
26	42	2.27415288-010	27	43	3.45272103-010

N	R	A COEFFICIENT	N	R	A COEFFICIENT
28	0	1.49445981-001	29	1	4.33393344+000
28	2	-6.08246064+001	29	3	-6.28421181+002
28	4	4.09557957+003	29	5	2.70230137+004
28	6	-1.08404618+005	29	7	-5.41807676+005
28	8	1.49473001+006	29	9	6.14199693+006
28	10	-1.23280570+007	29	11	-4.36837809+007
28	12	6.57950476+007	29	13	2.07375745+008
28	14	-2.38145795+008	29	15	-6.82210656+008
28	16	6.00431393+008	29	17	1.58818906+009
28	18	-1.06662464+009	29	19	-2.63639087+009
28	20	1.33118387+009	29	21	3.10347643+009
28	22	-1.14449045+009	29	23	-2.53552267+009
28	24	6.48241313+008	29	25	1.37297347+009
28	26	-2.20465235+008	29	27	-4.48637865+008
28	28	3.60917243+007	29	29	7.08551758+007
28	30	-1.09665393+006	29	31	-2.08208967+006
28	32	1.72947525+004	29	33	3.17919886+004
28	34	-1.79417961+002	29	35	-3.19662302+002
28	36	1.36355377+000	29	37	2.35686872+000
28	38	-8.07444899-003	29	39	-1.35519763-002
28	40	3.87776395-005	29	41	6.32504536-005
28	42	-1.55350501-007	29	43	-2.46452172-007
28	44	5.30154613-010	29	45	8.18627918-010

N	R	A COEFFICIENT	N	R	A COEFFICIENT
30	0	-1.44464448-001	31	1	-4.47839789+000
30	2	6.73205106+001	31	3	7.40429205+002
30	4	-5.19495360+003	31	5	-3.63560070+004
30	6	1.57935752+005	31	7	8.34528314+005
30	8	-2.51042445+006	31	9	-1.08740809+007
30	10	2.39955497+007	31	11	8.93956203+007
30	12	-1.49503101+008	31	13	-4.94247508+008
30	14	6.37970055+008	31	15	1.91279551+009
30	16	-1.92172116+009	31	17	-5.30965713+009
30	18	4.15323502+009	31	19	1.07038031+010
30	20	-6.46868427+009	31	21	-1.56985346+010
30	22	7.20473215+009	31	23	1.65898250+010
30	24	-5.60706230+009	31	25	-1.23258559+010
30	26	2.90826100+009	31	27	6.13456719+009
30	28	-9.14459540+008	31	29	-1.85878893+009
30	30	1.39504797+008	31	31	2.74225777+008
30	32	-3.96874799+006	31	33	-7.56049633+006
30	34	5.87332562+004	31	35	1.08543874+005
30	36	-5.72916751+002	31	37	-1.02809634+003
30	38	4.10168521+000	31	39	7.15306561+000
30	40	-2.29202285-002	31	41	-3.88764897-002
30	42	1.04043999-004	31	43	1.71770334-004
30	44	-3.94598254-007	31	45	-6.34531441-007
30	46	1.27666310-009	31	47	2.00099247-009

N	R	A COEFFICIENT	N	R	A COEFFICIENT
32	0	1.39949934=001	33	1	4.61834783+000
32	2	-7.40335815+001	33	3	=8.63631730+002
32	4	6.49032981+003	33	5	4.80188864+004
32	6	-2.24575488+005	33	7	=1.25086093+006
32	8	4.07490839+006	33	9	1.85571204+007
32	10	-4.46529093+007	33	11	=1.74482568+008
32	12	3.20812879+008	33	13	1.11000700+009
32	14	-1.59094578+009	33	15	=4.98250244+009
32	16	5.62669494+009	33	17	1.62094729+010
32	18	-1.44736972+010	33	19	=3.88283430+010
32	20	2.73307571+010	33	21	6.89360946+010
32	22	-3.78678436+010	33	23	-9.04961849+010
32	24	3.80659576+010	33	25	8.67327382+010
32	26	-2.70549478+010	33	27	=5.90788889+010
32	28	1.29416017+010	33	29	2.72019887+010
32	30	-3.78375412+009	33	31	=7.68348920+009
32	32	5.40413833+008	33	33	1.06348048+009
32	34	-1.44530808+007	33	35	=2.76150142+007
32	36	2.01478076+005	33	37	3.74102579+005
32	38	-1.85456708+003	33	39	=3.34916560+003
32	40	1.25497583+001	33	41	2.20592096+001
32	42	-6.63884135-002	33	43	=1.13662657=001
32	44	2.85709851-004	33	45	4.76777220-004
32	46	-1.02871601-006	33	47	=1.67428493-006
32	48	3.16396546-009	33	49	5.02544162=009

N	R	A COEFFICIENT	N	R	A COEFFICIENT
34	0	-1.35833760-001	35	1	-4.75418158+000
34	2	8.09569778+001	35	3	9.98378762+002
34	4	-8.00129893+003	35	5	-6.23996631+004
34	6	3.12595097+005	35	7	1.83048638+006
34	8	-6.41993982+006	35	9	-3.06641338+007
34	10	7.99065375+007	35	11	3.26779192+008
34	12	-6.55186519+008	35	13	-2.36784233+009
34	14	3.73128248+009	35	15	1.21837081+010
34	16	-1.52780970+010	35	17	-4.58133484+010
34	18	4.59829648+010	35	19	1.28205650+011
34	20	-1.03017556+011	35	21	-2.69668425+011
34	22	1.72540198+011	35	23	4.27367149+011
34	24	-2.15171723+011	35	25	-5.07516148+011
34	26	1.97033849+011	35	27	4.44885690+011
34	28	-1.28845819+011	35	29	-2.79732238+011
34	30	5.71835114+010	35	31	1.19822368+011
34	32	-1.56224913+010	35	33	-3.16960829+010
34	34	2.09750981+009	35	35	4.13173636+009
34	36	-5.29259918+007	35	37	-1.01389705+008
34	38	6.97329247+005	35	39	1.30020812+006
34	40	-6.07632838+003	35	41	-1.10352648+004
34	42	3.89819890+001	35	43	6.90030104+001
34	44	-1.95774350-001	35	45	-3.37988663-001
34	46	8.00933702-004	35	47	1.34943118-003
34	48	-2.74485082-006	35	49	-4.51578592-006
34	50	8.04496846-009	35	51	1.29312369-008

N	R	A COEFFICIENT
36	0	1.32060600-001
36	2	-8.80844695+001
36	4	9.74802417+003
36	6	-4.26977199+005
36	8	9.85167598+006
36	10	-1.38161449+008
36	12	1.28143276+009
36	14	-8.29715053+009
36	16	3.88797048+010
36	18	-1.35044001+011
36	20	3.52965446+011
36	22	-6.99421167+011
36	24	1.05159028+012
36	26	-1.19190637+012
36	28	1.00197418+012
36	30	-6.06665404+011
36	32	2.51110056+011
36	34	-6.43809679+010
36	36	8.15503809+009
36	38	-1.94765347+008
36	40	2.43270992+006
36	42	-2.01242628+004
36	44	1.22728722+002
36	46	-5.86661237-001
36	48	2.28715700-003
36	50	-7.47789577-006
36	52	2.09322877-008

Security Classification

DOCUMENT CONTROL DATA - R & D

(Security classification of title, body of abstract and indexing annotation must be entered when the overall report is classified)

1. ORIGINATING ACTIVITY *(Corporate author)*

Naval Research Laboratory
Washington, D.C. 20390

2a. REPORT SECURITY CLASSIFICATION

UNCLASSIFIED

2b. GROUP

3. REPORT TITLE

IMAGE ENHANCEMENT WITH PROLATE SPHEROIDAL WAVE FUNCTIONS

4. DESCRIPTIVE NOTES *(Type of report and inclusive dates)*

Interim report on one phase of the problem; work is continuing.

5. AUTHOR(S) *(First name, middle initial, last name)*

Henry A. Brown

6. REPORT DATE

November 29, 1968

7a. TOTAL NO. OF PAGES

56

7b. NO. OF REFS

11

8a. CONTRACT OR GRANT NO.

NRL Problem R02-14

b. PROJECT NO.

RF-05-151-402-4005

c.

d.

9a. ORIGINATOR'S REPORT NUMBER(S)

NRL Report 6798

9b. OTHER REPORT NO(S) *(Any other numbers that may be assigned this report)*

10. DISTRIBUTION STATEMENT

This document has been approved for public release and sale; its distribution is unlimited.

11. SUPPLEMENTARY NOTES

12. SPONSORING MILITARY ACTIVITY

Department of the Navy
(Office of Naval Research),
Washington, D.C. 20360

13. ABSTRACT

If the electric field intensity in the Fraunhofer region of a one-dimensional radiating source can be represented as a finite Fourier transform of the source current, then the source current can be reconstructed exactly by using prolate spheroidal wave functions and a segment of either the far field or the diffraction-limited image for the noise-free case. An example of the image enhancement of this process is given for the case of two equal point sources, which are unresolved in the Rayleigh sense. The point response function of this process shows that the resolution cell extent can be readily reduced to less than 10% of the Rayleigh cell with only 20 degrees of enhancement processing. A method of generating the Legendre polynomial and power series expansions of the prolate spheroidal angle functions of the first kind and order zero, $S_{0n}(c, x)$, has been worked out in detail. The Legendre polynomial expansion coefficients for degrees n = 0(1)40 and the power series expansion coefficients for degrees n = 0(1)36 are tabulated for $c = 2$.

DD FORM 1 NOV 65 1473 (PAGE 1)

S/N 0101-807-6801

Security Classification

Security Classification

14. KEY WORDS	LINK A ROLE	LINK A WT	LINK B ROLE	LINK B WT	LINK C ROLE	LINK C WT
Imaging						
Image enhancement						
Wave functions						
Resolution						
Resolution improvement						
Super resolution						
Rayleigh criterion						
Prolate spheroidal						
Wave functions						

DD FORM 1 NOV 65 1473 (BACK)
(PAGE 2)

Security Classification